Advances in Microstructural Diffusion Neuroimaging for Psychiatric Disorders

Ofer Pasternak[a,b], **Sinead Kelly**[a,c], **Valerie J. Sydnor**[a], and **Martha E. Shenton**[a,b,d]

[a.]Department of Psychiatry, Brigham and Women's Hospital, Harvard Medical School, Boston, MA.

[b.]Department of Radiology, Brigham and Women's Hospital, Harvard Medical School, Boston, MA.

[c.]Massachusetts Mental Health Center Public Psychiatry Division of the Beth Israel Deaconess Medical Center, Harvard Medical School, Boston, MA, United States

[d.]Veteran Affairs Boston Healthcare System, Brockton Division, Brockton, MA.

Abstract

Understanding the neuropathological underpinnings of mental disorders such as schizophrenia, major depression, and bipolar disorder is an essential step towards the development of targeted treatments. Diffusion MRI studies utilizing the diffusion tensor imaging (DTI) model have been extremely successful to date in identifying microstructural brain abnormalities in individuals suffering from mental illness, especially in regions of white matter, although identified abnormalities have been biologically non-specific. Building on DTI's success, in recent years more advanced diffusion MRI methods have been developed and applied to the study of psychiatric populations, with the aim of offering increased sensitivity to subtle neurological abnormalities, as well as improved specificity to candidate pathologies such as demyelination and neuroinflammation. These advanced methods, however, usually come at the cost of prolonged imaging sequences or reduced signal to noise, and they are more difficult to evaluate compared with the more simplified approach taken by the now common DTI model. To date, a limited number of advanced diffusion MRI methods have been employed to study schizophrenia, major depression and bipolar disorder populations. In this review we survey these studies, compare findings across diverse methods, discuss the main benefits and limitations of the different methods, and assess the extent to which the application of more advanced diffusion imaging approaches has led to novel and transformative information with regards to our ability to better understand the etiology and pathology of mental disorders.

Keywords

Corresponding author: Ofer Pasternak, Brigham and Women's Hospital, Harvard Medical School, 1249 Boylston Street, Boston, MA 02215. ofer@bwh.harvard.edu.

1. Introduction

Psychiatric disorders such as schizophrenia, major depression, and bipolar disorder have remained a conundrum for scientists since they were first defined more than a century ago. These debilitating disorders often occur at a young age, causing life-long difficulties that interfere with an individual's social, occupational and emotional functioning. While in other disorders, for example Multiple Sclerosis (Matthews et al., 2016; Popescu and Lucchinetti, 2016), Alzheimer's disease (Hyman et al., 2012) and Parkinson's disease (Dickson et al., 2009; Shulman et al., 2011), clear neuropathologies have been delineated, this has, unfortunately, not been the case for psychiatric disorders. In fact, the role of brain dysfunction in psychiatric pathology was not initially evident given the gross tools available for investigation, leading Plum (1972) to caution that those striving to make these disorders more tractable were wasting their time, as such efforts would lead to a "graveyard of neuropathologists" (Plum, 1972).

Schizophrenia, major depression, and bipolar disorder each present with characteristic patterns of emotional, cognitive, and social impairments, although there is some overlap in these domains of functioning across disorders. Schizophrenia is a severe mental illness typified by the presence of positive psychotic experiences (e.g., hallucinations, delusions, and thought disorders), negative symptoms (e.g., anhedonia, avolition, alogia, and flat affect), and cognitive impairments (attention, memory, and executive functioning deficits) (Fervaha et al., 2014a, 2014b; Ho et al., 1998; Lepage et al., 2014). The core feature of major depressive disorder (MDD) is depressed mood and a loss of interest in, or lack of ability to derive pleasure from, activities of daily living (Kennedy, 2008; Uher et al., 2014). Bipolar disorder (BD) is a disorder of severe mood dysregulation often characterized by recurring episodes of mania and depression, with more than 50% of individuals additionally presenting with mania-associated psychotic features (Dunayevich and Keck, 2000). BD can be further classified into bipolar disorder 1 (BD1) and 2 (BD2), with BD2 representing a less severe form of the illness wherein patients present with hypomania rather than mania (National Collaborating Centre for Mental Health UK, 2006). Given the high prevalence of these three disorders in the general population and the decreased life expectancy of 7–20 years associated with them (Chesney et al., 2014), there is a critical need for more efficacious, neurobiological-based treatments to be developed, though this is contingent upon an advanced understanding of the role of the brain in these disorders.

The development of neuroimaging tools such as computed tomography (CT), magnetic resonance imaging (MRI), and positron emission tomography (PET) introduced the ability to non-invasively investigate the brains of individuals with psychiatric disorders, as well as the possibility of identifying pathological signatures of these disorders. Surprisingly, and in contrast with histopathological studies, studies employing a diversity of imaging modalities have identified abnormalities in the brains of individuals with psychiatric illnesses (e.g., Duval et al., 2015; Frydman et al., 2016; Howes et al., 2009; Kubicki et al., 2007; Mulders et al., 2015; Sexton et al., 2009; Shenton et al., 2001; Vargas et al., 2013; Weyandt et al., 2013); these cumulative findings make it clear that abnormalities in the brain are common across psychiatric disorders. Nonetheless, none of these imaging studies have provided conclusive, robustly reproducible, and neurobiologically unambiguous findings of the nature

required for a true breakthrough in understanding the pathophysiology of these disorders, their diagnosis, and their treatment (e.g., Boksa, 2013; Farah and Gillihan, 2012; Linden, 2012; MacQueen, 2010).

Diffusion MRI is one of the most important technological advances for psychiatric research, and it has played a critical role in the discovery of brain abnormalities involved in these disorders (Kubicki et al., 2007; Kubicki and Shenton, 2014; Wheeler and Voineskos, 2014). While other imaging modalities focus on macroscopic volumetric or functional (e.g., metabolic and vascular) changes, diffusion MRI introduces the ability to study microstructural changes in brain tissue. To date, most diffusion MRI studies have focused specifically on white matter, using analysis methods such as diffusion tensor imaging (DTI), and there is a considerable body of work demonstrating that DTI measures are changed in psychiatric disorders (e.g., Chen et al., 2016; Ellison-Wright and Bullmore, 2009; Nortje et al., 2013; Clark et al., 2011; Seal et al., 2008). These DTI findings have led to new clinical hypotheses proposing that psychiatric disorders involve white matter abnormalities that result in neuronal miswiring and connectivity issues throughout the brain, which may partially explain some of the clinical symptomology associated with these disorders (uri - Blake et al., 2015; Friston, 2002).

In DTI studies of schizophrenia patients, white matter disruptions of lower FA and higher MD and RD are commonly identified, predominantly in fronto-temporal, interhemispheric, and thalamo-cortical regions (e.g., Ellison-Wright and Bullmore, 2009; Kelly et al., 2017). In bipolar disorder, common findings include lower FA and higher RD in white matter tracts connecting prefrontal cortical regions with anterior limbic structures (specifically those involved in emotion regulation), as well as alterations in temporal white matter, anterior corpus callosum and cingulum regions, the uncinate fasciculus, and the superior longitudinal fasciculus (Phillips and Swartz, 2014). Finally, commonly reported white matter DTI alterations in major depressive disorder include lower FA in tracts such as the inferior longitudinal fasciculus, the inferior fronto-occipital fasciculus, the posterior thalamic radiation, the superior longitudinal fasciculus (Murphy and Frodl, 2011), and interhemispheric fibers running through the genu and body of the corpus callosum (Liao et al., 2013). It is important to note that the extent and location of findings largely vary across different DTI studies. This variation, however, does not necessarily reflect a lack of DTI robustness. Rather, some variability likely arises due to neurobiological heterogeneity within overarching diagnostic categories, as well as due to heterogeneity in study designs and analysis methods, including dissimilarities in sample size, the selected population (e.g., stage of the disorder or diverse symptom profiles) and acquisition quality (e.g., resolution, number of diffusion images, magnetic field strength).

Although DTI measures appear to be sensitive to subtle brain changes that occur in psychiatric disorders, these measures are not specific to any single neuropathology, or to any disorder (G. Chen et al., 2016; Dong et al., 2017; O'Donnell and Pasternak, 2015). Further, although some clinical studies have attempted to relate DTI measures to white matter and myelin integrity, methodological studies have provided clearer evidence that such associations are unwarranted, given that DTI measures can be affected by a multitude of factors including fiber arrangement, axon density, partial voluming with surrounding tissue

(e.g., gray matter and CSF), tissue density, subject motion, and image resolution (Basser and Jones, 2002; Jones and Leemans, 2011; Mori and Zhang, 2006; Tournier et al., 2011). This methodological ambiguity/imprecision necessitates that advanced microstructural imaging methods be developed with the capacity to provide superior specificity to underlying pathologies.

In response to this need, more advanced diffusion acquisition and modeling approaches have been developed in recent years, and a number of studies have applied these new tools to the study of psychiatric disorders. These advanced methods focus on increasing sensitivity to subtle changes, as well as on producing new measures that can be more precisely linked to specific pathologies. The purpose of this review is to provide an up-to-date account of how advanced microstructural diffusion imaging methods, i.e., those that go beyond the DTI model, are being used to study psychiatric disorders. We acknowledge that the number of studies performed to date is not expansive, and thus a secondary purpose of our review is to construct a set of recommendations, based on the current literature, that may be useful to those planning to use advanced microstructural diffusion MRI approaches. We have limited our review to studies of schizophrenia, BD, and MDD, given the high prevalence and personal and economic burden of these disorders, and given the large body of DTI studies investigating these afflictions.

2. Methods

To locate articles of relevance that employ diffusion models that go beyond DTI, searches were conducted using PubMed, Web of Science, and Google Scholar. Keywords included all possible pairwise combinations of a psychiatric disorder plus an advanced diffusion method, for example (Schizophrenia or Depression or Bipolar Disorder) AND (generalized fractional anisotropy/gFA, kurtosis/DKI, free water/free water imaging, Q-ball imaging or Q-space imaging, neurite orientation and dispersion and density imaging/NODDI, permeability diffusivity imaging/PDI). Full and abbreviated forms of each method (as indicated above) were searched separately. The review was inclusive up to June 1, 2017. Review articles and case studies were not included. Searches using the aforementioned terms yielded a total of 37 articles that were included in this review (27 on schizophrenia, 3 on depression, and 9 on bipolar disorder, with some papers comparing two or more disorders). A list of all papers included in the review, as well as their key findings, can be found in Table 1.

2.1 Diffusion MRI models and acquisitions

2.1.1 Diffusion Tensor Imaging—Typical diffusion acquisition sequences that enable DTI analyses and are currently available on most MR platforms as off-the-shelf sequences tend to apply six (but often many more for a more robust fit) non-collinear diffusion gradients that sensitize the signal to water molecule displacements. The different gradient directions are acquired with gradient strength and timing that determine a factor called the b-value (Le Bihan et al., 1989), which, for white matter, has an optimal value of around 1,000 s/mm^2. Gradient directions that have the same b-value construct a single shell to which a smaller number of baseline measurements (b=0, i.e., gradients are turned off) are added. In DTI, the diffusion weighed images from a single shell acquisition are modeled as a function

of a single diffusion tensor (Basser et al., 1994). Each voxel is fitted separately, resulting in a single tensor per voxel that can be deconstructed into various measures based on the eigenvalues of the tensor (Pierpaoli and Basser, 1996). The most commonly reported DTI parameter is fractional anisotropy (FA) (Pierpaoli et al., 1996), i.e., the normalized variance of the eigenvalues, which has been (inappropriately) interpreted as a measure of white matter integrity, and occasionally as a measure of myelin integrity (Alba-Ferrara and de Erausquin, 2013). Other tensor-derived measures include mean diffusivity (MD; the average of the eigenvalues), axial diffusivity (AD; the largest eigenvalue), and radial diffusivity (RD; the average of the two minor eigenvalues); RD and AD are considered to be more specific to demyelination and axonal degeneration, respectively, than FA (Song et al., 2002). The main advantages of the DTI model are its sensitivity to subtle microstructural changes and its mathematical simplicity. This simplicity, however, is also its major shortcoming, as only a limited set of parameters is available for describing all of the potentially complicated changes that may occur in brain tissue. As a result, none of the DTI measures can truly serve as an index of white matter integrity (Jones et al., 2013) or any other specific pathology.

2.1.2 Advanced diffusion MRI methodologies—In our review of the literature we identified 7 different advanced diffusion MRI approaches that had been applied to data acquired from individuals with schizophrenia, BD, or MDD. These methods can be broadly clustered into two families—non-model based and model based approaches (Figure 1). The non-model based approaches steer away from the DTI model by analyzing properties of the signal itself that do not require the explicit assumption of an underlying model. The three non-model based approaches included in this review are q-space imaging, diffusion spectrum imaging (DSI), and diffusion kurtosis imaging (DKI).

The second family of approaches includes those that are model based. In these approaches, the single tensor model used in DTI is replaced or augmented with more elaborate models. These models attempt to better account for different biological processes that can affect the diffusion MRI signal, with the goal of defining parameters that are closer to the underlying tissue microstructure and to potential pathologies. These approaches typically involve defining compartments that represent distinct pools of water molecules, with each compartment being modeled separately. In this review, the model based approaches examined include: free-water imaging, permeability diffusivity imaging (PDI), neurite orientation dispersion and density imaging (NODDI), and q-space trajectory imaging (QTI).

Most advanced diffusion MRI models require acquisitions that are more complicated than the typical single-shell acquisition. These advanced acquisitions collect signal from gradient orientations that cover more than a single b-value, i.e., a multi-shell acquisition, where each shell sensitizes the signal to different ranges of displacement profiles. Some approaches utilize higher b-values (e.g., larger than 2,000 s/mm^2) where non-Gaussian diffusion profiles are extant (Assaf et al., 2002; Assaf and Cohen, 1998; Mulkern et al., 1999; Stanisz et al., 1997), thereby providing more information about restricted and hindered diffusion; this in turn allows for new parameters and supports more elaborate microstructural models. Technical details of the acquisition parameters used in the different papers reviewed here are in Table 2.

Below we review the 7 advanced diffusion MRI methods that have been used in studies of schizophrenia, MDD, and BD aimed at investigating microstructural parameters. We note that these methods by no means provide a complete account of all available advanced diffusion MRI methods. We additionally note that diffusion MRI is also useful for obtaining information about the orientation of white matter bundles, from which tractography and connectivity between different brain areas can be estimated. Nevertheless, because this is not necessarily related to local tissue microstructure, we have chosen to omit this from the review.

3.   A survey of advanced microstructural diffusion MRI studies in psychiatry

3.1   Non-model based approaches

3.1.1   Q-space imaging—The aim in diffusion imaging is to extract properties of the underlying diffusion profile. In DTI, this is done by assuming that the profile has a three-dimensional Gaussian distribution of displacements that can be parameterized by a diffusion tensor (Basser et al., 1994). In biological environments, however, the shape of the displacement often deviates from a Gaussian distribution (Novikov et al., 2011; Seroussi et al., 2017). For example, when diffusion is restricted (e.g., within white matter bundles) the displacement has a finite maximal distance (equivalent to the axon diameter), which is unlike a Gaussian distribution in which the mean squared displacement grows linearly with the diffusion time. In q-space imaging, the displacement distribution is approximated directly without assuming a certain distribution (Cohen and Assaf, 2002). To do this, the signal is collected in multiple b-values following a specific pattern (equally spaced q-values), which allows for the application of a Fourier transform, resulting in an approximation of the displacement distribution. While a direct estimation of the displacement distribution holds in it all of the diffusion properties, it is extremely difficult to properly estimate. In theory, it necessitates a very large number of different q-values reaching to very high q-values, which requires strong gradients and lengthy acquisition times, two requirements that are typically not available or feasible for clinical studies.

In a pilot study, Mendelsohn et al. (2006) conducted q-space imaging with 9 first episode schizophrenia patients and 5 healthy controls. They collected 16 b-values in 6 different orientations each, reaching to an extremely high b-value of 14,000 s/mm^2. Using a Fourier transform they estimated the displacement distribution, from which they extracted two measures of interest. The first measure is the apparent displacement, which represents the full width at half maximum of the displacement distribution function. In cases of free diffusion, this is proportional to the mean diffusivity. The second measure is the return to zero probability (i.e., the peak of the displacement function), which provides an indirect measure of restriction, with higher return to zero probability occurring in more restricted domains. Using a histogram analysis, Mendelsohn et al. (2006) observed a reduction in the return to zero probability and increased apparent displacement in individuals with schizophrenia. The return to zero probability also negatively correlated with the severity of positive and negative symptoms. White matter differences were prominent in severely ill patients, whereas in mildly ill patients there were no differences from controls. No

significant differences in FA were observed between patients and controls (MD was not compared).

Mendelsohn et al. (2006) concluded that the observed displacement differences were suggestive of altered white matter integrity in schizophrenia, and that high b-value data may provide a more direct measure of intra-axonal tissue and may thus be more suitable for studying early stages of brain pathology in schizophrenia. This early study demonstrates that measures derived from advanced diffusion imaging methods that are more closely related to neuronal tissue (return to zero probability) may offer increased sensitivity relative to DTI (FA). Regarding schizophrenia, this study presents preliminary results to suggest that more abnormalities exist in the brain than those identified by FA changes, and that co-occurring pathologies (at least two that are recognized here) may additionally exist. Obviously, the very small number of study participants challenges the robustness of these findings and limits our ability to appropriately gauge the potential of the q-space approach, which to date has not been replicated in a larger study. A clear limitation of this approach, however, is that the theory postulates that for an accurate estimation of the probability distribution, a much denser b- (or q-) value sampling is required. This is less feasible for human studies, especially those involving clinical populations. Methods that further develop q-space imaging (see below) attempt to resolve this limitation.

3.1.2 Diffusion spectrum imaging and generalized FA—Similar to the q-space approach, the diffusion spectrum imaging (DSI) approach acquires a dense sampling of the q-space in order to estimate the displacement function (Wedeen et al., 2005). DSI, however, attempts to estimate the function in 3D by obtaining a specific grid of b-values and orientations. In the literature, DSI has been primarily used for obtaining an estimation of the orientation distribution function (ODF) of white matter bundles, achieved by integrating over the orientations. A typical measure estimated from the resulting ODF is the generalized FA (gFA), which measures the anisotropy (i.e., the normalized standard deviation) of the ODF. gFA is thus similar to FA, although it is purported to provide a more direct measure of fiber bundle anisotropy, and to be less sensitive to errors that arise in the presence of complex fiber architectures, for example crossing and kissing fibers (Fritzsche et al., 2010; Gorczewski et al., 2009).

An alternative approach to extract the ODF from DSI data was introduced as q-ball imaging; in q-ball imaging a single high-b shell is sufficient to estimate the ODF (Tuch, 2004). There are several ways to approximate the ODF from such an acquisition, with the most popular approach being to model the diffusion signal with a spherical harmonics basis while applying regularization that reduces ODF estimation errors (Descoteaux et al., 2007).

Multiple studies have investigated whether gFA differs between psychotic patients and controls, with a subset examining correlations between gFA and clinical measures. In an early study investigating DSI-derived gFA measures along white matter tracts of the default mode network (DMN) in 12 patients with schizophrenia, Huang et al. (2010) found a negative correlation between functional connectivity of the inferior parietal lobe and the posterior cingulate gyrus/precuneus and the gFA of tracts connecting these regions (termed structural connectivity in the paper). They did not find a correlation between gFA and

symptom scores. In a follow up study, Huang et al. (2011) used the same approach to investigate the association between gFA and candidate schizophrenia vulnerability genes. A significant negative correlation was found between gene dosage and gFA in the posterior cingulate gyrus and the precuneus. A similar DSI acquisition was used by Wu et al. (2014) to investigate whether or not structural alterations in the language network are linked to auditory verbal hallucinations (AVHs) in 18 patients with schizophrenia and 18 controls. They reported that patients had significantly lower gFA in left ventral, right ventral, and right dorsal language tracts. The gFA values did not correlate with age, duration of illness, or clinical status. They also found a positive correlation between right dorsal pathway gFA and functional lateralization (measured with fMRI) of the dorsal pathway in patients, but not controls. Both right dorsal pathway gFA and functional lateralization negatively correlated with delusion/hallucination symptom scores, suggesting that greater gFA of right hemisphere language tracts may be linked to less severe language-related symptoms in schizophrenia.

In another DSI-derived gFA study, Wu et al. (2015b) employed an automated tractography-based analysis to investigate differences in white matter tracts across 31 patients with schizophrenia, 31 unaffected siblings, and 31 healthy controls. Significant group differences in gFA were found in the arcuate fasciculus, the fornix, auditory tracts, optic radiation, the genu of the corpus callosum, and callosal tracts connecting bilateral dorsolateral prefrontal cortices (DLPFC), temporal poles, and hippocampi. Post-hoc analyses revealed that the gFA of the right arcuate fasciculus was significantly decreased in both patients and unaffected siblings compared to controls, whereas gFA values for the nine other tracts were significantly decreased in patients only. There were no significant correlations between gFA and symptom scores. The authors thus concluded that the right arcuate fasciculus may be a candidate trait marker for genetic vulnerability to schizophrenia. Using the same approach in a sample of 31 chronic and 25 first episode patients with schizophrenia and 31 healthy controls, Wu et al. (2015a) found significant differences between groups in the arcuate fasciculus, the fornix, the superior longitudinal fasciculus, and corpus callosum fibers projecting to bilateral DLPFC, bilateral temporal poles, and bilateral hippocampi. Post-hoc between-group analyses revealed that in all of these tracts, gFA was reduced in both chronic and first episode patients as compared to controls, with the exception of callosal fibers connecting left and right DLPFC, which demonstrated reduced gFA in chronic, but not first episode, patients. There were no associations between gFA and clinical parameters. These results were interpreted as evidence for the existence of white matter structural alterations throughout the entire course of illness.

Tseng et al. (2015) used DSI to investigate white matter tracts of the mirror neuron system (MNS) in 32 schizophrenia patients and 32 controls. They found that patients displayed decreased mean gFA in fibers interconnecting bilateral pars opercularis as well as a negative correlation between gFA in these fibers and negative symptom scores. Other MNS tracts did not show significant gFA alterations. Griffa et al. (2015) used DSI to characterize the structural connectome in schizophrenia. Using a network-based structural connectivity analysis, they found a distributed set of brain regions that displayed altered nodal segregation or integration properties in 16 schizophrenia patients as compared to 15 controls, and furthermore showed that gFA values were significantly lower in schizophrenia patients

in tracts connecting affected brain nodes, yet not in those connecting unaffected nodes. Katz et al. (2016) compared white matter architecture in a sample of 23 individuals with high functioning autism, 24 patients with schizophrenia, and 32 healthy controls. Compared to controls, both autism and schizophrenia groups exhibited decreased gFA in the left fronto-occipital inferior fasciculus, possibly suggesting that similar neurostructural alterations may underlie language and social cognition impairments in both disorders. Finally, Baumann et al. (2016) used a DSI acquisition with a maximal b-value of 8,000 s/mm^2 to study the fornix in a sample of 42 early psychosis patients and 42 healthy controls, and found lower gFA in the fornix in patients.

Taken together, the aforementioned gFA studies consistently found reduced gFA in white matter in individuals with schizophrenia, and abnormalities were occasionally associated with disorder symptoms. These studies however typically had modestly sized samples as compared to recent DTI studies, and they unfortunately did not conduct comparisons with DTI measures in order to evaluate if the sensitivity of gFA is superior to that provided by DTI.

Rathi et al. (2010) used a different analytical approach, spherical harmonics, to calculate gFA and generalized norm (gN) from low b-value data (b=900). The gN, or the norm of the spherical harmonics coefficients, (inversely) represents the overall diffusion in the ODF. They compared gFA and gN with FA and norm obtained from a two-tensor model in 21 first episode schizophrenia patients and 20 healthy controls. In order to assess the sensitivity of these diffusion models for characterizing patients, they tested the classification accuracy of the different measures, ultimately concluding that isotropic parameters (gN and norm) outperformed parameters of anisotropy (gFA and FA). Furthermore, tensor based classifiers —a combination of FA, norm and mode—demonstrated better classification performance than spherical harmonics based classifiers, combining gFA and gN.

The gFA has also been assessed in a number of BD studies. With the intention of better characterizing white matter deficits throughout the entire brain in BD, Sarrazin et al. (2014) investigated mean gFA for 22 major white matter tracts in 118 individuals (obtained across three centers) with euthymic BD1, and 88 healthy controls. gFA was computed from a single shell acquisition using spherical harmonics decomposition. Compared to healthy controls, individuals with BD evinced decreased gFA in the left anterior arcuate fasciculus, the body and the splenium of the corpus callosum, and the long fibers of the left cingulum bundle. A secondary analysis of these three tracts comparing individuals with BD with and without psychotic features furthermore revealed that psychotic symptoms in BD were associated with lower gFA in the body of the corpus callosum. gFA was not correlated with duration of illness, medication load, or IQ. Despite the conventional single shell acquisition, DTI parameters were not reported.

In a study of frontal white matter tracts that included the corpus callosum, the cingulum, the uncinate fasciculus, and the inferior fronto-occipital fasciculus, Scholz et al. (2016) used a single shell acquisition to extract gFA from a spherical harmonics decomposition. They replicated findings in euthymic BD1 patients (n=24) of reduced gFA in the cingulum bundle, although in the right hemisphere, rather than the left as was found in Sarrazin et al. (2014).

The authors also investigated associations between gFA values and risk-taking behavior. Here, gFA of the right cingulum accounted for 25% of the variance in subject risk-taking behavior on The Cambridge Gambling Task, and a negative correlation between risky behavior on this task and gFA of the left inferior fronto-occipital fasciculus was reported in the BD group only. Again, DTI parameters were not reported.

Two studies (Favre et al., 2016; Souza-Queiroz et al., 2016) investigated whether or not mean gFA in the uncinate fasciculus was different between healthy controls and individuals with either BD1 or BD2. Interestingly, neither of these studies found a group difference in uncinate fasciculus gFA between healthy and patient groups, in accordance with studies by Sarrazin et al. (2014) and Scholz et al. (2016), but in contrast with the majority of DTI studies that examined FA in the uncinate fasciculus. Both Souza-Queiroz et al. (2016) and Favre et al. (2016) applied a single shell acquisition with b=1,400 (60 directions in Souza-Queiroz et al., 2016; 30 directions in Favre et al., 2016). Of note, Favre et al. (2016) also compared the gFA measure with MD, where they reported MD decreases along the left uncinate fasciculus following a psychoeducation program.

Canales-Rodríguez et al. (2014) also implemented a combined analysis of gFA and DTI measures (FA and MD) in 40 euthymic BD1 patients and 40 matched controls, to examine BD-related abnormalities in white and gray matter. Results from this whole brain analysis revealed decreased FA in the splenium of the corpus callosum and the right insula in BD, increased gFA in frontotemporal, subcortical, and cerebellar regions in BD, and widespread MD increases in patients, primarily in the cingulum, the left insula, and subcortical nuclei. Alterations in gFA and FA in the patient group did not overlap spatially, supporting the notion that these measures provide distinct but complimentary information about the brain. The authors also extracted a measure of return to zero probability, here termed probability to origin, (PTO, see Figure 2), which showed significant decreases in patients in the left insula, right lingual cortex, and cerebellum. Furthermore, gFA was sensitive to changes in the gray matter, whereas FA was not. According to the authors, FA was most sensitive for detecting abnormalities in white matter tracts consisting of parallel fibers (e.g., the corpus callosum), gFA was most sensitive to aberrations occurring in white matter structures with heterogeneously organized fibers, and MD was best able to detect global, non-specific changes in diffusion in both gray and white matter.

Studies utilizing gFA to investigate neuronal alterations in MDD are more scarce, however Chen et al. (2016) compared 16 MDD patients to 30 healthy controls by acquiring data with a multi-shell acquisition and extracting gFA. They also extracted two additional parameters, including normalized quantitative anisotropy (NQA), an alternative measure of anisotropy extracted from the peaks of the ODF, and the isotropic value of the ODF, which is the smallest diffusion in any direction, equivalent to DTI's RD. The authors reported a decrease in gFA and NQA in the superior longitudinal fasciculus and an increase in the isotropic component in the frontal lobe in MDD patients. In the corpus callosum, NQA correlated with Hamilton Depression Rating Scale scores, and gFA correlated with the Hospital Anxiety and Depression Scale scores. The authors hypothesized that their findings may point to two different pathologies: that gFA and NQA changes may be due to white matter integrity loss, and that the isotropic change may arise from reduced neuronal size or glial

density. However, this hypothesis was not directly supported by additional evidence in the paper.

Overall, it appears that gFA studies tend to parallel previous FA findings. In almost all instances, previous DTI studies have found FA decreases in the same locations as reported gFA decreases. The variability across different studies in terms of the extent and location of changes in gFA also suggests that the heterogeneity of FA findings is not necessarily improved by using gFA. On the other hand, when directly comparing gFA and FA from the same data (Canales-Rodriguez et al. 2014), alterations in the two measures do not appear to overlap spatially. This lack of overlap supports the notion that these measures may provide complimentary information about the brain. Importantly, Canales-Rodriguez et al. (2014) reported that the sensitivity of gFA was lower than that of FA, and that gFA changes were limited to areas of complex fiber architecture, i.e., locations where the FA measure is understood to be less accurate.

The studies by Rathi et al. (2010), Favre et al. (2016), Canales-Rodriguez et al. (2014) and Chen et al. (2016) may additionally attenuate the potential importance of the gFA measure as they demonstrate that isotropic measures were more sensitive to group differences than the gFA measure. These studies, in conjunction with studies evincing that FA and gFA changes arise in areas with different fiber architectures, raise the concern that investigations that only assess gFA (e.g., single high b-value data from which DTI measures cannot be extracted) may fail to identify some abnormalities that conventional DTI would identify.

In summary, the gFA measure substantiated previous results obtained using DTI, but it has yet to provide new, transformative information about psychiatric disorder pathophysiology. On the other hand, the DSI studies that compared multiple diffusion parameters arrived at conclusions similar to that derived from the q-space study: that psychiatric disorders appear to involve two different pathologies, one that affects anisotropy and is potentially related to the microstructural arrangement of the tissue, and a second that affects diffusivity or the degree of restriction, likely related to changes in the microstructural composition of the tissue itself.

3.1.3 Diffusion kurtosis imaging—When water molecules are diffusing in a restricted domain, their displacement profile deviates from a Gaussian distribution. Kurtosis (or, more accurately, the excess kurtosis) is a mathematical term that measures how much a distribution deviates from being Gaussian. Kurtosis can be measured directly from an estimated displacement function, though an alternate way to estimate it that requires fewer measurements is to deconstruct the signal from multiple b-values and directions into its cumulant expansion (Jensen et al., 2005). The first order of the expansion is a constant, the second order is a function of a diffusion tensor, and the next order, which quantifies kurtosis, is a function of a fourth order tensor. Several types of kurtosis parameters can be estimated, and depending on the desired parameters, different acquisition protocols are required. The typical acquisition used in clinical studies consists of two shells, a b>=2,000 and a b=~1,000, in addition to a few b=0 images, although optimal acquisitions may have many more shells and much higher b-values (Jensen et al., 2005; Zhu et al., 2015). Scalar measures can also be extracted from the kurtosis tensor, including mean kurtosis (MK), axial

kurtosis (AK) and radial kurtosis (RK), in addition to DTI parameters (FA, MD, etc.), which can be extracted from the diffusion tensor. Kurtosis imaging does not, however, use a biological model to represent the data. Rather, these metrics reflect how the restricted diffusion manifests in 3D space, and are thus indicators of microstructural restriction. Kurtosis is currently the most frequently utilized advanced diffusion MRI method outside of the mental health literature, and altered kurtosis values have been found in a variety of neurological disorders, including stroke (Jensen et al., 2011), cancer (Raab et al., 2010), Alzheimer's disease (Fieremans et al., 2013), epilepsy (Gao et al., 2012), and Parkinson's disease (Kamagata et al., 2013).

In a preliminary study with a small sample of 10 patients with schizophrenia and 8 controls, Ramani et al. (2007) conducted a histogram analysis of the prefrontal cortex (PFC), demonstrating that individuals with schizophrenia had reduced FA and reduced MK in PFC white matter voxels. The authors concluded that the observed alterations might reflect axonal degeneration and a possible loss of oligodendrocytes in the white matter of this region, although such a conclusion, without additional supporting evidence, is likely an over interpretation. Notably, the between-group difference in MK histograms was greater than that seen in the FA analysis, suggesting higher sensitivity for MK. The analysis of MD showed no significant group differences, although this may be due to the extremely small size of the sample, which greatly limits the robustness of these findings.

Zhu et al. (2015) compared DKI and DTI measures in 94 schizophrenia patients and 91 sex- and age-matched healthy controls. Using a two-shell acquisition (with 25 directions for both b=1,000 and b=2,000 shells) and tract-based spatial statistics (TBSS) to assess group differences, the authors found (Figure 3) that DTI-derived diffusion parameters (RD, FA and MD) detected abnormalities in white matter regions with coherent fiber arrangements (e.g., the corpus callosum and the anterior limb of internal capsule), whereas kurtosis parameters (MK and AK) detected differences in white matter regions with complex fiber arrangements (e.g., the corona radiata and white matter adjacent to the cortex). Importantly, these findings imply that typical DTI metrics are more sensitive to alterations occurring along bundles of fibers that run in parallel, whereas DKI measures appear to have increased sensitivity in regions with branching or crossing fibers, similar to the gFA studies reported above. Diffusion and kurtosis parameters thus appear to provide complementary information, given their differing sensitivities to Gaussian and non-Gaussian diffusion profiles, and investigations seeking to identify the full spectrum of microstructural abnormalities should consider using them jointly.

Using the same acquisition as in their aforementioned 2015 paper, Zhu et al. (2016) used DKI to estimate FA in a sample of 19 schizophrenia patients with severe delusions, 30 schizophrenia patients without delusions, and 30 healthy controls. Patients without delusions had lower FA in the body of the corpus callosum and the superior corona radiata in comparison to healthy controls. In comparison to patients with severe delusions, patients without delusions additionally had lower FA in the inferior longitudinal fasciculus and the optic radiation. These findings surprisingly suggest that schizophrenia patients with severe delusions have comparable FA to normal. Alternatively, they may speak to the fact that looking at the relationship between just one clinical feature (e.g., delusions) and diffusion

imaging parameters very likely does not capture the complex relationship that exists between clinical presentation and underlying brain microstructure. It is interesting to note that despite acquiring a DKI acquisition, the authors only reported on DKI-derived FA, choosing not to report findings involving kurtosis-specific measures of MK, AK, and RK, or other tensor derived parameters (e.g., MD).

In another study with a similar acquisition protocol, Narita et al. (2016) compared DTI and kurtosis measures in a sample of 31 patients with schizophrenia and 31 controls. In comparison to FA measures, more widespread MK reductions were observed in schizophrenia; MK reductions were observed in the limbic lobe, frontal lobe, parietal lobe, bilateral superior longitudinal fasciculi, and the right corona radiata. Left superior longitudinal fasciculus MK values also significantly negatively correlated with the severity of positive symptoms. No significant correlations between FA and clinical measures were observed, demonstrating that kurtosis measures were, in this study, more sensitive for detecting associations with schizophrenia symptomology, as well as for identifying group differences in white matter microstructure.

Docx et al. (2017) used DKI (MK) in comparison with DTI (MD and FA) to investigate the association between white matter microstructure and volitional motor activity in a sample of 20 patients with schizophrenia and 16 healthy controls. Following family-wise error rate correction, there were no group differences in MK and FA values between patients and controls, and only limited brain regions evinced increased MD in patients. However, in the patient group, greater motor activity positively correlated with MK in the inferior, middle, and superior longitudinal fasciculi, the corpus callosum, the posterior fronto-occipital fasciculus, and the posterior cingulum. This study might be less robust than the ones reported above due to the smaller sample size, and we caution against attributing changes in motor activity solely to kurtosis changes in these white matter tracts. Nevertheless, this study does provide further support to the idea that non-Gaussian measures are more likely to correlate with symptoms or behavioral pathologies.

Finally, in a DKI study of the cerebellum in BD, unipolar depression, and healthy controls (Figure 4), both DTI and DKI parameters identified differences between unipolar depression patients and controls in the white matter of the superior and middle cerebellar peduncles, as well as between BD patients and controls in the middle cerebellar peduncles. However, when comparing patients with unipolar depression and BD, only the DTI parameter MD was significantly different (in cerebellar white matter). In contrast, in the gray matter of the dentate nuclei, MK was the only measure that differentiated BD from the other two groups (Zhao et al., 2016). This report demonstrates that combining DKI and DTI parameters maximizes the sensitivity of the DKI approach, and it demonstrates a utility for DKI in gray matter.

Findings from the collection of DKI papers reviewed above reveal the importance of combining DKI-derived parameters of FA, AD, RD and MD with kurtosis specific measures (MK, AK, RK) in order to detect a greater range of abnormalities. More specifically, kurtosis measures appear to provide increased sensitivity to group differences that occur in areas with complex fiber arrangements, as well as, potentially, in gray matter. So far, the

main contribution of these kurtosis analyses to the mental health literature is in extending the white matter locations that may be affected into areas of complicated fiber arrangements, thus evincing that more areas are affected than previously suspected. Kurtosis findings also suggest that the MK measure may be more related to the actual underlying disease pathology than FA as it better correlates with clinical measures, though it should be noted that there was no overlap in the clinical measures that correlated with MK, indicating that it may be more pathologically, but not clinically, specific.

3.2 Model based approaches

3.2.1 Free-water Imaging—Free-water imaging is a model-based approach (Pasternak et al., 2009) that augments the DTI model by including a second compartment that accounts for the contribution of free-water throughout the brain; free-water is defined as water molecules that do not experience hindrance or restriction during the experiment time. When using a typical diffusion MRI acquisition, the diffusion time dictates that free-water in the brain can only be expected in larger extracellular spaces, such as in cerebrospinal fluid (CSF), interstitial water, or plasma. The free-water compartment is modeled as isotropic with a fixed diffusion coefficient of water in body temperature (3×10^{-3}mm^2/s). The second compartment (the tissue compartment) uses the DTI model, i.e., it is modeled using a single diffusion tensor. By eliminating extracellular free-water, tissue compartment DTI measures are inherently corrected for free-water (e.g., CSF) contamination. The parameters estimated in this model are: 1) the fractional volume of the free-water compartment (FW), which quantifies the contribution of extracellular free-water to the signal and changes during processes such as ventricle size change, atrophy, edema and chronic neuroinflammation (Pasternak et al., 2016; Syková and Nicholson, 2008); and 2) the diffusion tensor of the tissue compartment, from which scalar measures such as tissue-FA (FA_T) are calculated. Due to the elimination of CSF contamination, the FAT measure is expected to be more specific than traditional FA to changes that occur within neuronal tissue (Metzler-Baddeley et al., 2012). Free-water measures can be obtained from single-shell data by applying regularization, which assumes continuity between neighboring voxels. The model can also be estimated from multi-shell data (Hoy et al., 2014; Pasternak et al., 2012), in which case the regularization assumptions can be relaxed.

Pasternak et al. (2012) first compared free-water and DTI measures in a cohort of 18 first episode patients and 20 controls. Using the conventional DTI model, widespread decreased FA and increased MD were found in patients compared to healthy individuals (Figure 5). After correcting for free-water, however, the FA measure no longer showed a widespread group difference (Figure 5). Rather, FA_T differences were limited to regionally specific areas, mainly to frontal lobe white matter. The FW measure, on the other hand, exhibited global increases in patients, which overlapped with the MD and FA findings. These results suggested that the majority of group differences seen in FA in this first episode population were actually driven by increased extracellular free-water, rather than by tissue-related changes. The authors proposed that this may point to two separate pathologies in early schizophrenia, one that affects the cellular domain, such as axonal degeneration, and a second, more extensive pathology that affects the extracellular domain, potentially neuroinflammation.

Lyall et al. (2017) replicated this finding of spatially limited FA_T decreases and whole brain FW increases in a study of 63 first episode patients and 70 controls. In this paper, the FW measure in first episode patients was positively correlated with performance on the MATRICS Consensus Cognitive Battery following 12 weeks of antipsychotic treatment. Lyall et al. (2017) proposed a hypothesis wherein FW is indicative of a heightened neuroimmune response in the primary stages of schizophrenia, with this initial response being associated with a gain of functionality in terms of cognitive functioning. In a follow-up study of 29 chronic schizophrenia patients and 25 matched controls, the extent of elevated FW in schizophrenia patients was found to be limited, while FA_T reductions were largely pervasive. More specifically, there was an approximately 200% increase in the number of white matter skeleton voxels that exhibited reduced FA_T in this study of chronic patients, when compared to findings from Pasternak et al. (2012) in first episode patients.

These studies indicate that extracellular changes play a role in the early stages of schizophrenia, and that, as the disease progresses, there is an increased presence of tissue abnormalities. Oestreich et al. (2017) corroborated these findings using a multi-site cohort of 281 chronic schizophrenia patients and 188 controls. They reported primarily reduced FA_T in the anterior limb of the internal capsule bilaterally, the posterior thalamic radiation bilaterally, as well as the genu and body of the corpus callosum. In this large study, there were no significant FW changes. Contrary to this study, in a multi-modal analysis Mandl et al. (2015) used magnetization transfer ratio (MTR) in conjunction with free-water imaging in a sample of 40 chronic schizophrenia patients and 40 healthy controls, but did not identify significant group differences in any of the free-water imaging diffusion parameters (including FA_T). Of note, the data in this study as well as in the Oestreich et al. (2017) study were acquired on 1.5T scanners, which may suggest inferior sensitivity that requires a larger sample size (such as that used by Oestreich et al. (2017)) for a significant finding. Finally (Wang et al., 2016) compared 81 at-risk for mental state subjects and 36 controls, and found reduced FA_T in the left cingulum, left side of the corpus callosum, left uncinate fasciculus, forceps minor, left inferior fronto-occipital fasciculus, left superior longitudinal fasciculus, and left anterior thalamic radiation. FA_T in the forceps minor was significantly more reduced in subjects who later developed psychosis as compared to those who did not. Symptom severity, as measured by CAARMS total severity score, was correlated with decreased FA_T within the left inferior fronto-occipital fasciculus, the left uncinate fasciculus, and the left anterior thalamic radiation in at-risk subjects. This study suggests sensitivity to abnormalities even prior to psychosis onset. However, in this study FW was not evaluated, and the FA_T results were not compared with FA results.

Differences in white matter microstructure and extracellular free-water were also associated with state and trait delusions in an investigation of 87 chronic schizophrenia patients and 28 controls. Oestreich et al. (2016) observed that the presence of both state and trait (currently remitted) delusions were associated with reduced FA_T and increased RD_T in left and right cingulum bundles, while increased extracellular free-water in the left cingulum bundle, specifically, was associated with present (state) delusions. In this same study, the authors noted the lack of significant group differences in diffusion measures in the fornix and the uncinate fasciculus, two limbic tracts commonly found to exhibit differences in schizophrenia in the literature. They suggested that correcting FA for the presence of free-

water likely removes the bias of partial volume that may have influenced findings observed in previous DTI studies.

Interestingly, a study of 17 individuals with BD1 and 28 controls reported that individuals with chronic bipolar disorder look most similar to schizophrenia patients in their first episode, in that the chronic BD group showed global FW increases, but no significant FA_T decreases, compared to controls (Tuozzo et al., 2017). Tuozzo et al. (2017) interpreted these findings as indicative of a globalized acute response, possibly inflammation, in BD. No correlations were found between free-water measures and clinical scores, however, suggesting that changes in extracellular free-water do not impact clinical presentation, but rather reflect an up- or down-stream process related to the central neuropathology of the disorder.

The utility of the free-water model in psychiatric research has additionally been examined in MDD. In a study of 18 healthy individuals and 17 diagnosed with MDD, Bergamino et al. (2016) performed a voxel-wise analysis to compare groups using both DTI (FA, AD, RD) and free-water corrected DTI measures (FA_T, AD_T, RD_T). Although group comparisons using traditional DTI metrics revealed no significant differences between the two groups, after applying a free-water correction individuals with MDD evinced decreased FAT and ADT in overlapping regions of the left inferior fronto-occipital fasciculus. ADT values in the MDD group were also significantly negatively correlated with stress measures derived from the Perceived Stress Scale and the Penn State Worry Questionnaire. The increased sensitivity of free-water corrected measures was substantiated experimentally using a bootstrapping procedure, which supported that there was a robust difference between using free-water corrected versus uncorrected measures with regards to between-group effect sizes in FA and AD, and neural-behavioral correlations. This underscores the potential importance of removing partial volume effects and extracellular CSF contamination from the diffusion signal.

Considered together, the primary contribution of these free-water imaging studies appears to be their ability to distinguish between two disparate pathologies that can both account for similar changes in conventional DTI measures. Additionally, the studies support the notion that correcting for CSF contamination improves the ability to uncover subtle anomalies in brain microstructure in psychiatric disorders. The discovery of the development of extracellular and cellular pathologies at different stages along the progression of schizophrenia and BD could be transformative to our understanding of the etiology of these disorders, as this challenges current DTI-based theories proposing that widespread demyelination or axonal degeneration exists in the early stages of disease. Instead, free-water imaging studies reveal that extracellular processes may be more closely related to psychosis onset.

Still, despite free-water imaging's ability to model two separate compartments, it remains equivocal as to what biological changes drive changes in each compartment. Although it has been suggested that neuroinflammation may be the source of increases in the extracellular compartment, the extracellular space can also be affected by atrophy, axonal density changes, and other parameters such as motion and temperature.

3.2.2   Permeability diffusivity imaging (PDI)—The permeability diffusivity imaging (PDI) model is a variant of a two compartment diffusion model, based on theoretical work by Sukstanskii et al. (2004, 2003). This model suggests that the bi-exponential decay of the diffusion signal reflects the permeability of cellular membranes, as opposed to two physical compartments. PDI estimates and quantifies the effect of permeable barriers on diffusion as the ratio between the diffusivity of two water pools, i.e., D_r/D_u, where D_r is the diffusivity of the restricted pool and Du is the diffusivity of the unrestricted pool (Figure 6). The model also estimates the fraction of the signal that comes from each pool. The unrestricted pool represents water molecules that are far away from axonal walls and other water barriers, whereas the restricted pool is formed by water that is close to cellular walls and diffusivity barriers and thus more likely to undergo either passive exchange (diffusion) across cell membranes and/or active exchange via ionic water pumps (Baslow, 2002). According to this model, small changes in the permeability of the axon or cell membrane predominantly affect the restricted diffusion pool coefficient (Dr), thus making PDI sensitive to membrane permeability differences (Sukstanskii et al., 2003, 2004). Lower permeability may represent less-efficient water exchange via axonal ion channels and water pores of the axonal membrane (Nilsson et al., 2013). Estimating the model requires an extensive multi-shell protocol that is based on the q-space imaging protocol. The protocol includes 15 b-value shells with 30 directions per shell and a maximal b-value of 3,800 s/mm^2. Due to this intense acquisition protocol, only a limited field of view can be acquired in a reasonable time frame. In the studies listed below, that field of view covers the mid-sagittal portion of the corpus callosum and the cingulate.

Kochunov et al. (2013) acquired data using a PDI protocol from 26 schizophrenia patients and 26 controls. They observed significantly lower D_r and PDI (D_r/D_u) in the corpus callosum and cingulate gray matter of patients, as well as more modest differences in FA in these regions. There were no group differences in axial or radial diffusivity, in D_u, or in the fractional volumes of the PDI compartments. PDI and FA were significantly correlated in patients. The authors suggested that reduced cross-membrane water molecule exchange, potentially a marker of ion channel abnormalities, could explain the observed reductions in FA, although they could not provide a clear biological mechanism that would explain the positive correlation between the measures.

Using the same data with additional subjects added, Kochunov et al. (2014) tested whether accelerated age-related decline in schizophrenia was related to a greater volume of hyperintensive white matter (HWM) lesions or to reduced PDI. In the larger sample of 40 controls and 30 patients, they found once again that patients had significantly lower corpus callosum PDI and FA, with a significant age-by-diagnosis interaction. No differences in HWM volume were observed. The accelerated decline in FA seen in schizophrenia patients was also explained by a decline in PDI. The authors therefore deduced that PDI may be a more sensitive measure of schizophrenia-related white matter deficits.

In Kochunov et al. (2016), the PDI values obtained from the corpus callosum were compared with DKI and DTI values obtained from a sample of 74 schizophrenia patients, 41 healthy siblings, and 113 healthy controls. The authors observed significant differences between patients ‖ and controls across four measures (FA, kurtosis anisotropy (KA), axial kurtosis

(K‖), and PDI); three of these measures (FA, KA, and PDI) showed significant differences between controls and the siblings of schizophrenia patients as well. Combining the three measures by applying principal component analysis, the outcome composite measures explained patient–control differences in processing speed, but not differences in working memory or psychiatric symptoms; this same association was found for the healthy siblings of the patients. The authors concluded that non-Gaussian measures may better capture the association between white matter and core cognitive deficits in individuals with schizophrenia and their first-degree relatives.

In these three PDI studies, PDI abnormalities overlapped with FA abnormalities, yet the PDI measure resulted in larger effect sizes when differentiating between groups. The preliminary inference that can be made, with the significant caveat of limitations discussed below, is that FA changes typically found in the corpus callosum in schizophrenia studies may be caused by a decrease in membrane permeability. This is potentially a transformative finding in schizophrenia, as it introduces a new candidate pathology that necessitates further investigation. The PDI model presents a few limitations however. First, the model assumes that any change in diffusivity can ultimately be explained by a change in permeability (assuming that the restricted and non-restricted diffusivities are not changing at exactly the same rate). This assumption has not yet been proven, and it is probable that other factors, including axon diameter and CSF contamination, also affect diffusivities, independent of permeability. Second, the model assumes that the restricted diffusion in high-b value shells can be modeled by a Gaussian process, an assumption that is contrary to most other high-b methods, which model restricted diffusion using models such as cylinders or sticks. Lastly, this model requires extensive acquisition time that limits coverage to only a few slices, thus with the current acquisition this methodology may not be practical for clinical studies that seek to examine multiple regions of the brain. As a result of these limitations it is difficult to identify a biological mechanism that elucidates the relationships found between PDI and other diffusivity measures. Due to this difficulty, the authors of Kochunov et al. (2016) suggested that the derived diffusion metrics should primarily be discussed in a phenomenological way without referring to specific biological postulations.

3.2.3 Neurite orientation dispersion and density imaging (NODDI)—The
Neurite orientation dispersion and density imaging (NODDI) approach (Zhang et al., 2012) estimates a three compartment model (Figure 7)—intracellular, extracellular, and free-water compartments. Similar to the free-water model, the free-water compartment is modeled as isotropic with the diffusion coefficient of water in body temperature. The intracellular compartment models the space bounded by the membranes of neurites (axons and dendrites). It is modeled as a set of cylinders with zero radius (sticks), simulating the highly restricted diffusion perpendicular to the neurites. Diffusion parallel to the sticks is set to a constant of 1.7×10^{-3} mm^2/s. The orientation of the sticks is dispersed according to a mathematical function. In the original implementation, a Watson distribution is used that has two free parameters, the mean orientation of the neurites and the orientation dispersion about that mean. The fractional volume of the intracellular compartment is used as an estimate of neurite density. The extracellular compartment models the space around the neurites. Given that the extracellular space is hindered and not restricted, this compartment

is parametrized using a distribution of tensors that are assumed to have the same orientation dispersion as the intracellular sticks. The parallel and radial diffusivity of the tensors are set as a function of the parallel diffusivity of the sticks, the neurite density, and the neurite dispersion. Accordingly, the model has the following free parameters: the neurite density (ND) parameter, the orientation dispersion index (ODI), the free-water fraction, and the mean orientation of the neurites.

Since the NODDI model deviates from the Gaussian model, it requires a multi-shell acquisition with both high b-values (e.g., 2,000–2,500 s/mm^2) and b-value shells in the range of b=1,000. An optimal acquisition includes 2 shells, a 30-direction shell with a b-value of about 700 s/mm^2 and a 60-direction shell with a b-value of about 2,000 s/mm^2, however the model can be fitted from similar acquisitions as well. NODDI provides a way to identify if microstructural changes in brain tissue are caused by ND changes, or by ODI changes. The ND measure could be a sensitive yet nonspecific marker of demyelination, indicative of a pathological neurodegenerative process. The ODI parameter is a marker of banding and fanning of axons, which may provide insight into neurodevelopmental pathologies (Crow et al., 2007; Savadjiev et al., 2014).

Rae et al. (2017) used NODDI measures (ODI and ND), as well as DTI measures (FA and MD), to assess microstructural differences between 35 first episode psychosis patients and 19 healthy controls. TBSS analyses revealed that patients in their first episode of psychosis had lower regional FA in multiple commissural, corticospinal, and association tracts. They found (Figure 8) that the differences in FA predominantly co-localized with regions of reduced ND, rather than with the ODI, a measure of aberrant fiber bundle arrangement. Therefore, the authors suggested that neurite density differences may contribute to white matter aberrations in early psychosis, highlighting the utility of non-Gaussian measures for explaining traditional DTI metrics.

Relevant to this review, Nazeri et al. (2016) applied NODDI to model gray matter microstructural properties in 36 schizophrenia patients, 29 patients with BD1, and 35 healthy controls. They observed significantly lower gray matter ND in the temporal pole, the anterior parahippocampal gyrus, and the hippocampus in schizophrenia patients in comparison to the healthy controls. No significant differences in gray matter ND were observed between patients with BD1 and schizophrenia patients or healthy controls. Regardless of diagnosis, spatial working memory performance was significantly associated with higher gray matter ND. The authors also discussed the potential utility of ND for biological subtyping in psychiatry, an area which should be further explored.

We note that neither the Rae et al. (2017) study nor the Nazeri et al. (2016) study reported whether or not there were any findings with the extracellular component that was extracted fromm NODDI.

In summary, the NODDI model is similar to the free-water model in that it eliminates CSF contamination, though it goes further by separating changes in the tissue into two possible factors, neurite orientation or neurite density changes. The model, however, is limited by some of its assumptions, the main one being that the diffusivities of the tissue compartments

are fixed. While this assumption may hold for healthy brains, it is not clear whether or not it remains valid for brains with pathologies. In fact, a recent paper by Lampinen et al. (2017) suggests that this assumption may bias the estimation of neurite density in healthy brains as well. In this paper (Lampinen et al., 2017), an alternative acquisition approach (described below in section 3.2.4) was used to demonstrate how a more accurate estimation of neurite orientation dispersion and neurite density can be performed. Given the small number of studies that have used NODDI in psychiatry, it is still quite early to predict if NODDI will play an important role in unraveling the etiology of psychiatric disorders. For now, it brings up an interesting candidate, neurite density, as having a potential role in disorder pathophysiology.

3.2.4 Q-space trajectory imaging (QTI)—Q-space trajectory imaging is a very recent model and acquisition approach (Westin et al., 2016), first applied clinically to schizophrenia. This method was developed to improve the discrimination of sizes, shapes, and orientations of diffusion within tissue. QTI changes the way the diffusion signal is acquired by replacing the pulsed gradient with a free form gradient that rotates in q-space. The effect of this measurement is that the signal is sensitized to water molecule displacement in all orientations simultaneously; instead of collecting separate gradient directions, the signal is sensitized to the sequential orientation displacement of each water molecule. For example, molecules that are within an anisotropic domain will yield a different signal from those in an isotropic domain, even if these anisotropic domains are randomly ordered and macroscopically isotropic (Figure 9). Similar to conventional pulsed gradient acquisitions, the free-form gradient properties can be described using a group of parameters, which in QTI is collected into a second order tensor called the b-tensor rather than to the familiar b-value. Collecting data with several b-tensor shapes and sizes is equivalent to the collection of multiple-shell data, and it provides a collection of signal that is sensitive to different orders and kinds of displacements.

To quantify microstructure from QTI, Westin et al. (2016) suggested a model of infinite microenvironments, where each microenvironment is Gaussian. By decomposing this model into its cumulant expansion, a function that depends on a diffusion tensor, a 4th order tensor is obtained. This is similar to kurtosis imaging, except that the measures now represent microscopic features rather than macroscopic features. Westin et al. (2016) proposed a family of rotationally invariant scalar quantities describing microstructural features derived from the 4th order tensor, which include microscopic anisotropy (shape variability), dispersion (orientation variability), and size variability.

Measuring QTI from a small sample of 5 healthy controls and 5 patients with schizophrenia, Westin et al. (2016) observed that 9 out of the 14 parameters investigated showed significant differences between groups. The authors concluded that the ability to model the distribution of diffusion tensors within a single voxel might be more powerful in capturing complex white matter architecture, as opposed to quantities that have already been averaged within a voxel. Based on this small pilot study, it is too early to evaluate the current contribution of QTI to the study of schizophrenia or other mental disorders. Nonetheless, QTI will be highly relevant for future analyses, especially given that the method is capable of providing the

same type of information (except, arguably, more accurate) that the kurtosis imaging and NODDI methods provide.

4. Discussion

To date, only a limited number of investigations have applied advanced diffusion MRI techniques to the study of psychiatric disorders. Nonetheless, available studies have begun to offer interesting insights into psychiatric neuropathology from which early conclusions can be drawn.

The most readily drawn conclusion is that advanced diffusion MRI methods continue to observe the trend set by diffusion tensor imaging: that brain abnormalities are consistently found in psychiatric populations. While this may partially reflect selective reporting and an unwillingness or inability to publish negative findings, it still undoubtedly supports the notion that subtle neurobiological abnormalities are present in white matter (and likely in gray matter) in psychiatric patients. Authors of the reviewed papers provide two main reasons for employing more advanced diffusion imaging methods as opposed to conventional DTI. The first reason is to increase methodological sensitivity to brain abnormalities, and the second reason is to attempt to provide a better explanation as to the source of these abnormalities.

Of the 7 methods reviewed, gFA and DKI are the two methods most focused on increasing the sensitivity of DTI by replacing existing DTI parameters with measures that are presumed to be more directly related to tissue microstructural changes (especially those that occur in white matter). It is, nonetheless, difficult to assess whether or not the gFA measure is more sensitive than DTI FA, given that most studies did not directly compare these two measures. Nevertheless, Canales-Rodríguez et al's (2014) important study established that the gFA measure improves the capacity to identify abnormalities in areas of complex fiber architecture. gFA does not, however, appear to improve the detection of abnormalities in the rest of the white matter, and it may actually be less sensitive than FA in many regions. Moreover, the gFA measure is not sensitive to isotropic changes that consistently appear in psychiatric disorders. For these reasons, we suggest that gFA may not, on its own, be sufficient for characterizing and understanding the nature of brain abnormalities in psychiatry. We recommend that whenever possible, the standard DTI model should be applied alongside advanced diffusion MRI methods. This will help to increase overall sensitivity while simultaneously helping to evaluate the added benefits (or lack thereof) that these new measures provide.

Unlike gFA analyses, the DKI analysis inherently estimates DTI parameters, and therefore many of the DKI studies reviewed reported changes in both kurtosis-derived DTI and DKI measures. This is an advantage of the DKI model, since, in theory, it can only contribute additional information to the DTI model. Indeed, from the papers reviewed, it appears that a combination of kurtosis and diffusivity measures provides higher sensitivity than that of DTI measures alone. Additionally, DKI measures may be more closely linked to disorder symptomatology. It should be noted, however, that DKI requires higher b-values with lower

signal to noise ratios, and thus DKI is often collected with a lower resolution than optimized DTI protocols, which might reduce some of DKI's sensitivity as compared to DTI.

With regards to specificity, authors of both gFA and DKI studies argue that the derived measures are more specific to white matter pathologies. In many of the reviewed papers, gFA is used as a proxy for microstructural integrity, and DKI measures are considered to be directly representative of a demyelination index. From the studies reviewed here, it is not yet clear whether the interchangeable use of these imaging and biological terms is justified. The specificity of kurtosis, for example, is limited by its susceptibility to partial volume effects such as CSF contamination, and by the fact that in complex architecture, macroscopic averaging yields isotropic profiles that are less useful to characterize microscopic anisotropy.

The free-water imaging, PDI, and NODDI methods reviewed here aim to improve the specificity of DTI measures to particular and distinctive pathologies. Interestingly, these three methods assume three different explanations for decreases in FA. Free-water imaging has shown that FA decreases can be explained by either (or by a combination of) an increase in the isotropic extracellular fractional volume, or by a decrease in anisotropy in the vicinity of tissue. The PDI model attributes decreases in FA to changes in permeability, which seem to be driven (at least in schizophrenia) mainly by a decrease in the diffusivity of the restricted compartment. Lastly, the NODDI model explains decreases in FA as decreases in neurite density (i.e., the fraction of the restricted compartment). These differences merit further direct comparisons between these methods in the same sample.

The different ways in which these three models interpret findings of decreased FA highlight two interesting limitations of model based approaches: 1) It is difficult to assess whether the more complicated models over fit the signal variability or truly represent underlying microstructural changes, though if findings continue to be replicated this will lend support to the later. When variability in the signal exists, this variability has to be absorbed by one of the free parameters of the model. In the free-water imaging model, the variability can be absorbed by either the fractional volume of the extracellular space, or by the diffusivity/FA of the tissue compartment. In the PDI model, the variability can be absorbed by either a change in permeability (as estimated by the ratio of restricted and non-restricted diffusivities) or by the fractional volume of the restricted compartment. In the NODDI model, the variability can be absorbed by the fractional volume of the extracellular space, by the neurite dispersion, or by the neurite density. And 2) The model is only as good as its underlying assumptions. While these models are mathematically advanced and biologically feasible, here it is clear that some assumptions from different models are also contradictory. For example, free-water imaging assumes that there is no permeability, whereas PDI aims to quantify permeability directly, presuming that this is the main explanation for observable group differences. The PDI model additionally operates under the assumption that there is no extracellular free-compartment, and it can thereby be biased by CSF contamination, a bias that can alter the biological interpretation of the PDI parameter. Along similar lines, the NODDI model explicitly assigns a fixed restricted diffusivity, which PDI has shown to be the main parameter that differentiates schizophrenia patients from healthy controls. Finally, PDI and free-water imaging assume a single fiber orientation, whereas NODDI allows for a distribution of orientations in order to explain signal variability. Unfortunately, the scope of

this review does not allow us to conclude which of these assumptions is most valid. This, along with techniques that lessen the chance of overfitting (e.g., regularization and cross validation) are critical areas of investigation for future studies, given the compelling hypotheses that each model engenders.

The conclusion that follows is that parameters derived from advanced models are likely quite sensitive (and likely more sensitive than DTI) to brain abnormalities, yet, while improving the specificity of DTI, they are still not definitively specific to individual pathologies. This continued lack of specificity must be considered by users trying to interpret the results of any given model. Moreover, the explicit names chosen for some model parameters increase the likelihood of confusion in their interpretation, whereby, for example, a change in the permeability diffusivity index does not necessarily signify a change in permeability, and a change in the neurite density parameter can occur due to changes other than in neurite density. Adding to the danger of misinterpretation is the application of these advanced methods to studies with small cohorts. Such studies are important as proof of concept, but physiological interpretation of their results should be avoided until a) results are replicated in larger and more robustly designed studies, and b) the neurobiological bases of derived parameters are further investigated and validated.

Validation studies using post-mortem histological analyses, animal models, or other techniques (e.g. phantoms or simulated data) that can link imaging findings to specific pathologies are key for understanding and justifying the use of certain diffusion measures. These studies will be central to interpreting transformative diffusion findings in the mental health literature, and will mitigate many over interpretation concerns. Some preliminary work has been done in this direction, for example in relating kurtosis measures with histopathology (Hui et al., 2008; Umesh Rudrapatna et al., 2014), with reactive astrogliosis (Zhuo et al., 2012) in rat brains, and with demyelination in mouse brains (Falangola et al., 2014; Jelescu et al., 2016). Similarly, preliminary histopathological studies are also available for DSI/gFA (Shen et al., 2015), and for NODDI measures (Sato et al., 2017).

The aforementioned studies are important validation studies for diffusion MRI methods, yet the vast majority of validation studies have looked at neurological disorders, i.e., disorders with known pathologies that can be reliably induced and identified in animal models. Discerning the specificity of a diffusion measure to a relevant candidate pathology and ascertaining the role of that pathology in producing disorder symptoms is much more difficult for psychiatric than for neurological illnesses. This is since it is still largely unclear what pathologies may indeed be "relevant" to investigate or induce (which is why developing hypotheses from neuroimaging studies is critical), and because human pathology (both biological and psychological) may not be readily comparable to animal models. Human post-mortem studies offer an alternative solution, though these are typically conducted on chronically ill subjects, thus brains may primarily show signs of illness chronicity and medication use, rather than indicators of the initial pathology of interest.

Despite the limitations of model based approaches and the current need for validation, these methods remain superior to most proposed since the conception of *in vivo* neuroimaging. As such, there is much to be gained by employing these approaches, especially when there is a

need to differentiate between what are likely two distinct pathologies. Accordingly, the major contribution of these model based studies is the understanding that there are often two or more co-occurring pathologies contributing to the etiology of a single psychiatric disorder. An additional important conclusion is that the spatial distributions of these pathologies may change (and interact) over the lifetime course of a disorder, offering insight into different stages of illness. As an example, the free-water imaging studies in schizophrenia have provided evidence of two co-occurring pathologies, one that is extracellular and isotropic that manifests in the early stages of schizophrenia, and a second affecting the tissue that is more prominent in the later stages of the disorder. This finding is paralleled in other advanced method studies reviewed here that investigated isotropic processes. The discovery of this isotropic effect early in the disease course has led to investigations into the possible pathological underpinnings of extracellular diffusion changes, using other tools such as PET imaging and histological approaches. Sources currently being investigated include neuroinflammation, density changes, and permeability changes.

4.1 Recommendations for future studies

4.1.1 Study design—In the future, an important consideration for the application of any advanced diffusion MRI study will be the study design. More specifically, the selection of appropriate and more homogenous psychiatric sub-populations increases the likelihood of identifying abnormalities that correlate with clinical or cognitive measures, making it easier to relate imaging findings to specific, clinically-relevant symptoms or behaviors. Homogeneity may be achieved by studying genders separately, by limiting age ranges, and by including subjects in similar disorder stages with similar symptomatology. In turn, established diffusion imaging markers may contribute to alternative subtype definitions that focus more on dimensional traits rather than dichotomous classification, as was, for example, proposed by the Research Domain Criteria (RDoC) framework (Insel et al., 2010); this identification of biological subtypes may prove critical to our understanding of disorder risk and treatment. As described in our review, the advanced diffusion MRI measures often exhibited improved correlation with clinical and cognitive symptoms when directly compared to DTI measures, hence they may fit well within the RDoC framework. However, due to the large number of potential clinical and cognitive variables that are pertinent in psychiatry, care must be taken to reduce erroneous (i.e., false positive) findings by properly correcting for multiple comparisons. To avoid false negatives on the other hand, studies should be appropriately powered.

The large variability across studies (in factors such as design, symptomatic population, imaging sequences, sample sizes, preprocessing steps, and statistical analyses) likely contributes more to the variability seen in these advanced diffusion study results than the occurrence of false positives or false negatives. Clearly, surveying the spatial extent of the different abnormalities reported here (see Table 3) does not present a coherent picture of the brain areas that are afflicted. What is needed then are more studies that employ similar designs and analyses on homogenous populations, as this will allow for a more direct comparison of results. Longitudinal follow up studies will also be essential for understanding the dynamics of reported neurological aberrations; none of the studies

reviewed here followed subjects over time with multiple imaging sessions. Moreover, multi-modal imaging studies that integrate imaging information across modalities and with other clinical, cognitive, and biological (e.g., genetic, neuroendocrine, and blood-based) measures will be integral to the pursuit of developing a more comprehensive understanding of the pathologies that underlie these imaging abnormalities. For example, a promising approach could be to combine information from diffusion analyses with morphometric analyses from anatomical images, especially because collective morphometric findings reveal that a large number of abnormal patterns can be expected in mental disorders (Gupta et al., 2015).

In the future, more resources must also be devoted to the acquisition of large neuroimaging cohorts. The average statistical power of neuroimaging studies is very low, resulting in an overestimation of effect sizes as well as problems with the reproducibility of findings. In recent years, the neuroimaging community has seen the proliferation of multisite collaborations in a concerted effort to increase sample sizes and yield more robust estimates of effects for DTI studies (as well as other imaging modalities). These efforts are also needed for advanced diffusion MRI methods. Modification of retrospective meta-analysis tools such as those proposed by the ENIGMA-DTI workgroup (Jahanshad et al., 2013; Kochunov et al., 2015) could be an effective way to combine advanced diffusion data analyses. Users must be aware, however, that all of the diffusion metrics reviewed here are likely affected by scanner differences and scanner calibrations, even when the same make and model are used in different locations (Mirzaalian et al., 2016). Efforts to harmonize the acquired diffusion signal for combining multiple DTI datasets derived from different acquisition protocols can additionally be extended to advanced diffusion MRI methodologies, thereby allowing for joint analyses across different sites. For example, a recent method proposed by Mirzaalian et al. (2016) takes into account region-specific differences in the acquired signal from different scanners in order to harmonize the signal at each site in comparison to a reference site, using several rotation invariant spherical harmonic features.

4.1.2 Data acquisition—It is important to note that the different methods reviewed here require different acquisitions. All of the advanced methods reviewed require multi-shell acquisitions for an ideal estimation. However, the free-water imaging parameters and the gFA parameter can also be obtained from a single-shell acquisition. Based on the papers reviewed here, we offer the opinion that a DKI-like acquisition is destined to be the most general and simultaneously cost-effective sequence that will additionally allow for the estimation of most parameters discussed here, including DTI parameters, gFA, return-to-zero probability, DKI parameters, free-water imaging parameters, and NODDI parameters. A more ideal acquisition, however, would be similar to a DKI design with the addition of a few low b-value shells. The addition of these shells allows for better estimation of fast diffusing components that typically go unaccounted for and thereby bias the estimation of diffusion measures, for example vascular contributions (Rydhög et al., 2017) that are likely involved in many brain disorders. Of course, adding diffusion directions and b-values does increase the acquisition time. However, immerging technologies such as multi-band (Setsompop et al., 2016), compressed sensing (Michailovich et al., 2011), and super-

resolution (Ning et al., 2016) may considerably shorten the required time, making the more advanced diffusion methods much more feasible to acquire.

We also note that although the QTI acquisition may actually be the most general, QTI sequences are not yet available as a product on MRI vendors. Nevertheless, protocols similar to QTI approaches show promise, given that they allow for a more direct estimation of permeability (Lasi et al., 2011). These protocols are expected to have high clinical utility as they provide a feasible approach to simultaneous estimation of all of the candidate pathologies described throughout this review, including extracellular contributions, permeability, neurite density, and orientation dispersion.

5. Conclusions

As evinced in this review, much progress is being made towards developing and implementing methods that increase the degree of sensitivity and specificity of diffusion MRI, using both non-model based and multi-compartment model based approaches. Although none of the methods reviewed were specifically designed for examining psychiatric disorders, these newer methods nonetheless presented novel findings and offered new insight into psychiatry in at least two important ways: 1) Improved sensitivity allowed for the identification of microstructural white matter abnormalities outside of homogenous fiber areas, such as in areas with complex fiber arrangements, and possibly in gray matter; and 2) Increased specificity allowed for the detection of co-occurring pathologies that typically affect DTI- derived diffusion measures in the same way, and thus previously could not be distinguished.

Although the exact neurobiological sources of these co-occurring abnormalities remain to be fully elucidated, there are now new candidate pathologies that have the potential to explain the etiology and symptomatology of psychiatric disorders. These include pathologies that change the extracellular volume (e.g., inflammation), density changing pathologies (e.g., excessive pruning or degeneration), and permeability changing pathologies (e.g., membrane/ channel deficiencies). These important advances in disorder insight have emerged from just the small selection of studies reviewed here, warranting their application in future work. Future work is also needed, however, in order to validate the underlying assumptions of specific models, or else to establish evidence-based models designed to investigate specific candidate psychiatric related pathologies.

Our recommendation for future studies is to collect multi-shell diffusion data with both high and low b-values from which parameters derived from numerous different models can be estimated. Importantly, such data will also allow for a direct comparison of different advanced methods in the same clinical population. New study designs should emphasize the careful selection of clinical sub-populations, large cohorts, longitudinal imaging follow ups, and multidimensional data.

Future progress demands the integration of multi-modal imaging methods with behavioral, computational, neuroendocrine, neuroimmunological, and genetic approaches. The time is ripe for investigations such as these, given the invaluable potential that diffusion imaging

holds for elucidating neurological abnormalities at the core of these psychiatric disorders, and for further improving disorder diagnosis, risk-evaluation, and treatment through the implementation of neuroimaging-informed psychiatric evaluation and management.

Acknowledgments

References

Alba-Ferrara LM, de Erausquin GA, 2013 What does anisotropy measure? Insights from increased and decreased anisotropy in selective fiber tracts in schizophrenia. Front. Integr. Neurosci 7, 9 10.3389/fnint.2013.00009 [PubMed: 23483798]

Assaf Y, Ben-Bashat D, Chapman J, Peled S, Biton IE, Kafri M, Segev Y, Hendler T, Korczyn AD, Graif M, Cohen Y, 2002 High b-value q-space analyzed diffusion-weighted MRI: application to multiple sclerosis. Magn. Reson. Med 47, 115–126. [PubMed: 11754450]

Assaf Y, Cohen Y, 1998 Non-mono-exponential attenuation of water and N-acetyl aspartate signals due to diffusion in brain tissue. J. Magn. Reson. San Diego Calif 1997 131, 69–85. 10.1006/jmre.1997.1313

Baslow MH, 2002 Evidence supporting a role for N-acetyl-L-aspartate as a molecular water pump in myelinated neurons in the central nervous system. An analytical review. Neurochem. Int 40, 295–300. [PubMed: 11792458]

Basser PJ, Jones DK, 2002 Diffusion-tensor MRI: theory, experimental design and data analysis - a technical review. NMR Biomed 15, 456–467. 10.1002/nbm.783 [PubMed: 12489095]

Basser PJ, Mattiello J, LeBihan D, 1994 MR diffusion tensor spectroscopy and imaging. Biophys. J 66, 259–267. 10.1016/S0006-3495(94)80775-1 [PubMed: 8130344]

Baumann PS, Griffa A, Fournier M, Golay P, Ferrari C, Alameda L, Cuenod M, Thiran J-P, Hagmann P, Do KQ, Conus P, 2016 Impaired fornix–hippocampus integrity is linked to peripheral glutathione peroxidase in early psychosis. Transl. Psychiatry 6, e859 10.1038/tp.2016.117 [PubMed: 27459724]

Bergamino M, Pasternak O, Farmer M, Shenton ME, Hamilton JP, 2016 Applying a free-water correction to diffusion imaging data uncovers stressrelated neural pathology in depression. NeuroImage Clin 10, 336–342. 10.1016/j.nicl.2015.11.020 [PubMed: 27006903]

Boksa P, 2013 A way forward for research on biomarkers for psychiatric disorders. J. Psychiatry Neurosci. JPN 38, 75–77. 10.1503/jpn.130018 [PubMed: 23422052]

Canales-Rodriguez EJ, Pomarol-Clotet E, Radua J, Sarro S, Alonso-Lana S, Del Mar Bonnin C, Goikolea JM, Maristany T, Garcia-Alvarez R, Vieta E, McKenna P, Salvador R, 2014 Structural abnormalities in bipolar euthymia: a multicontrast molecular diffusion imaging study. Biol. Psychiatry 76, 239–248. 10.1016/j.biopsych.2013.09.027 [PubMed: 24199669]

Chen G, Hu X, Li L, Huang X, Lui S, Kuang W, Ai H, Bi F, Gu Z, Gong Q, 2016 Disorganization of white matter architecture in major depressive disorder: a meta-analysis of diffusion tensor imaging with tract-based spatial statistics. Sci. Rep 6, srep21825. 10.1038/srep21825

Chen VC, Shen CY, Liang SH, Li ZH, Tyan YS, Liao YT, Huang YC, Lee Y, McIntyre RS, Weng JC, 2016 Assessment of abnormal brain structures and networks in major depressive disorder using morphometric and connectome analyses. J. Affect. Disord 205, 103–111. 10.1016/j.jad.2016.06.066 [PubMed: 27423425]

Chesney E, Goodwin GM, Fazel S, 2014 Risks of all-cause and suicide mortality in mental disorders: a meta-review. World Psychiatry Off. J. World Psychiatr. Assoc. WPA 13, 153–160. 10.1002/wps.20128

Clark KA, Nuechterlein KH, Asarnow RF, Hamilton LS, Phillips OR, Hageman NS, Woods RP, Alger JR, Toga AW, Narr KL, 2011 Mean diffusivity and fractional anisotropy as indicators of disease and genetic liability to schizophrenia. J. Psychiatr. Res 45, 980–988. 10.1016/j.jpsychires.2011.01.006 [PubMed: 21306734]

Cohen Y, Assaf Y, 2002 High b-value q-space analyzed diffusion-weighted MRS and MRI in neuronal tissues - a technical review. NMR Biomed 15, 516–542. 10.1002/nbm.778 [PubMed: 12489099]

Crow TJ, Paez P, Chance SA, 2007 Callosal misconnectivity and the sex difference in psychosis. Int. Rev. Psychiatry Abingdon Engl 19, 449–457. 10.1080/09540260701486282

ur i -Blake B, van der Meer L, Pijnenborg GHM, David AS, Aleman A, 2015 Insight and psychosis: Functional and anatomical brain connectivity and selfreflection in Schizophrenia. Hum. Brain Mapp 36, 4859–4868. 10.1002/hbm.22955 [PubMed: 26467308]

Descoteaux M, Angelino E, Fitzgibbons S, Deriche R, 2007 Regularized, fast, and robust analytical Q-ball imaging. Magn. Reson. Med 58, 497–510. 10.1002/mrm.21277 [PubMed: 17763358]

Dickson DW, Braak H, Duda JE, Duyckaerts C, Gasser T, Halliday GM, Hardy J, Leverenz JB, Del Tredici K, Wszolek ZK, Litvan I, 2009 Neuropathological assessment of Parkinson's disease: refining the diagnostic criteria. Lancet Neurol 8, 1150–1157. 10.1016/S1474-4422(09)70238-8 [PubMed: 19909913]

Docx L, Emsell L, Van Hecke W, De Bondt T, Parizel PM, Sabbe B, Morrens M, 2017 White matter microstructure and volitional motor activity in schizophrenia: A diffusion kurtosis imaging study. Psychiatry Res 260, 29–36. 10.1016/j.pscychresns.2016.10.002

Dong D, Wang Y, Chang X, Jiang Y, Klugah-Brown B, Luo C, Yao D, 2017 Shared abnormality of white matter integrity in schizophrenia and bipolar disorder: A comparative voxel-based meta-analysis. Schizophr. Res 185, 41–50. 10.1016/j.schres.2017.01.005 [PubMed: 28082140]

Dunayevich E, Keck PE, 2000 Prevalence and description of psychotic features in bipolar mania. Curr. Psychiatry Rep 2, 286–290. [PubMed: 11122970]

Duval ER, Javanbakht A, Liberzon I, 2015 Neural circuits in anxiety and stress disorders: a focused review. Ther. Clin. Risk Manag 11, 115–126. 10.2147/TCRM.S48528 [PubMed: 25670901]

Ellison-Wright I, Bullmore E, 2009 Meta-analysis of diffusion tensor imaging studies in schizophrenia. Schizophr. Res 108, 3–10. 10.1016/j.schres.2008.11.021 [PubMed: 19128945]

Falangola MF, Guilfoyle DN, Tabesh A, Hui ES, Nie X, Jensen JH, Gerum SV, Hu C, LaFrancois J, Collins HR, Helpern JA, 2014 Histological correlation of diffusional kurtosis and white matter modeling metrics in cuprizoneinduced corpus callosum demyelination. NMR Biomed 27, 948–957. 10.1002/nbm.3140 [PubMed: 24890981]

Farah MJ, Gillihan SJ, 2012 The Puzzle of Neuroimaging and Psychiatric Diagnosis: Technology and Nosology in an Evolving Discipline. AJOB Neurosci 3, 31–41. 10.1080/21507740.2012.713072 [PubMed: 23505613]

Favre P, Houenou J, Baciu M, Pichat C, Poupon C, Bougerol T, Polosan M, 2016 White Matter Plasticity Induced by Psychoeducation in Bipolar Patients: A Controlled Diffusion Tensor Imaging Study. Psychother. Psychosom 85, 58–60. 10.1159/000441009 [PubMed: 26610264]

Fervaha G, Foussias G, Agid O, Remington G, 2014a Impact of primary negative symptoms on functional outcomes in schizophrenia. Eur. Psychiatry 29, 449–455. 10.1016/j.eurpsy.2014.01.007 [PubMed: 24630742]

Fervaha G, Foussias G, Agid O, Remington G, 2014b Motivational and neurocognitive deficits are central to the prediction of longitudinal functional outcome in schizophrenia. Acta Psychiatr. Scand 130, 290–299. 10.1111/acps.12289 [PubMed: 24850369]

Fieremans E, Benitez A, Jensen JH, Falangola MF, Tabesh A, Deardorff RL, Spampinato MVS, Babb JS, Novikov DS, Ferris SH, Helpern JA, 2013 Novel white matter tract integrity metrics sensitive to Alzheimer disease progression. AJNR Am. J. Neuroradiol 34, 2105–2112. 10.3174/ajnr.A3553 [PubMed: 23764722]

Friston KJ, 2002 Dysfunctional connectivity in schizophrenia. World Psychiatry Off. J. World Psychiatr. Assoc. WPA 1, 66–71.

Fritzsche KH, Laun FB, Meinzer H-P, Stieltjes B, 2010 Opportunities and pitfalls in the quantification of fiber integrity: what can we gain from Q-ball imaging? NeuroImage 51, 242–251. 10.1016/j.neuroimage.2010.02.007 [PubMed: 20149879]

Frydman I, de Salles Andrade JB, Vigne P, Fontenelle LF, 2016 Can Neuroimaging Provide Reliable Biomarkers for Obsessive-Compulsive Disorder? A Narrative Review. Curr. Psychiatry Rep 18, 90 10.1007/s11920-016-0729-7 [PubMed: 27549605]

Gao Y, Zhang Y, Wong C-S, Wu P-M, Zhang Z, Gao J, Qiu D, Huang B, 2012 Diffusion abnormalities in temporal lobes of children with temporal lobe epilepsy: a preliminary diffusional kurtosis imaging study and comparison with diffusion tensor imaging. NMR Biomed 25, 1369–1377. 10.1002/nbm.2809 [PubMed: 22674871]

Gorczewski K, Mang S, Klose U, 2009 Reproducibility and consistency of evaluation techniques for HARDI data. Magma N. Y. N 22, 63–70. 10.1007/s10334-008-0144-0

Griffa A, Baumann PS, Ferrari C, Do KQ, Conus P, Thiran J-P, Hagmann P, 2015 Characterizing the connectome in schizophrenia with diffusion spectrum imaging. Hum. Brain Mapp 36, 354–366. 10.1002/hbm.22633 [PubMed: 25213204]

Gupta CN, Calhoun VD, Rachakonda S, Chen J, Patel V, Liu J, Segall J, Franke B, Zwiers MP, Arias-Vasquez A, Buitelaar J, Fisher SE, Fernandez G, van Erp TGM, Potkin S, Ford J, Mathalon D, McEwen S, Lee HJ, Mueller BA, Greve DN, Andreassen O, Agartz I, Gollub RL, Sponheim SR, Ehrlich S, Wang L, Pearlson G, Glahn DC, Sprooten E, Mayer AR, Stephen J, Jung RE, Canive J, Bustillo J, Turner JA, 2015 Patterns of Gray Matter Abnormalities in Schizophrenia Based on an International Megaanalysis. Schizophr. Bull 41, 1133–1142. 10.1093/schbul/sbu177 [PubMed: 25548384]

Ho B-C, Nopoulos P, Flaum M, Arndt S, Andreasen NC, 1998 Two-Year Outcome in First episode Schizophrenia: Predictive Value of Symptoms for Quality of Life. Am. J. Psychiatry 155, 1196–1201. 10.1176/ajp.155.9.1196 [PubMed: 9734542]

Howes O, Egerton A, Allan V, McGuire P, Stokes P, Kapur S, 2009 Mechanisms underlying psychosis and antipsychotic treatment response in schizophrenia: insights from PET and SPECT imaging. Curr. Pharm. Des 15, 2550–2559. [PubMed: 19689327]

Hoy AR, Koay CG, Kecskemeti SR, Alexander AL, 2014 Optimization of a free water elimination two-compartment model for diffusion tensor imaging. NeuroImage 103, 323–333. 10.1016/j.neuroimage.2014.09.053 [PubMed: 25271843]

Huang S, Liu CM, Hwu H, Liu CC, Lin F, Tseng W, 2011 Correlating Functional and Structural Connectivity of Default Mode Network with Dosage of Two Candidate Vulnerability Genes of Schizophrenia. Proc Intl Soc Mag Reson Med 19.

Huang S, Yeh F, Hwu H, Liu CM, Liu CC, Lin F, Tseng W, 2010 Functional and Structural Connectivity of Default Mode Network in Patients with Schizophrenia: A Combined Resting-State fMRI and Diffusion Spectrum Imaging Study. Proc Intl Soc Mag Reson Med

Hui ES, Cheung MM, Qi L, Wu EX, 2008 Towards better MR characterization of neural tissues using directional diffusion kurtosis analysis. NeuroImage 42, 122–134. 10.1016/j.neuroimage.2008.04.237 [PubMed: 18524628]

Hyman BT, Phelps CH, Beach TG, Bigio EH, Cairns NJ, Carrillo MC, Dickson DW, Duyckaerts C, Frosch MP, Masliah E, Mirra SS, Nelson PT, Schneider JA, Thal DR, Thies B, Trojanowski JQ, Vinters HV, Montine TJ, 2012 National Institute on Aging–Alzheimer's Association guidelines for the neuropathologic assessment of Alzheimer's disease. Alzheimers Dement. J. Alzheimers Assoc 8, 1–13. 10.1016/j.jalz.2011.10.007

Insel T, Cuthbert B, Garvey M, Heinssen R, Pine DS, Quinn K, Sanislow C, Wang P, 2010 Research domain criteria (RDoC): toward a new classification framework for research on mental disorders. Am. J. Psychiatry 167, 748–751. 10.1176/appi.ajp.2010.09091379 [PubMed: 20595427]

Jahanshad N, Kochunov PV, Sprooten E, Mandl RC, Nichols TE, Almasy L, Blangero J, Brouwer RM, Curran JE, de Zubicaray GI, Duggirala R, Fox PT, Hong LE, Landman BA, Martin NG, McMahon KL, Medland SE, Mitchell BD, Olvera RL, Peterson CP, Starr JM, Sussmann JE, Toga AW, Wardlaw JM, Wright MJ, Hulshoff Pol HE, Bastin ME, McIntosh AM, Deary IJ, Thompson PM, Glahn DC, 2013 Multi-site genetic analysis of diffusion images and voxelwise heritability analysis: a pilot project of the ENIGMA-DTI working group. NeuroImage 81, 455–469. 10.1016/j.neuroimage.2013.04.061 [PubMed: 23629049]

Jelescu IO, Zurek M, Winters KV, Veraart J, Rajaratnam A, Kim NS, Babb JS, Shepherd TM, Novikov DS, Kim SG, Fieremans E, 2016 In vivo quantification of demyelination and recovery using compartment-specific diffusion MRI metrics validated by electron microscopy. NeuroImage 132, 104–114. 10.1016/j.neuroimage.2016.02.004 [PubMed: 26876473]

Author Manuscript Author Manuscript Author Manuscript Author Manuscript

Jensen JH, Falangola MF, Hu C, Tabesh A, Rapalino O, Lo C, Helpern JA, 2011 Preliminary observations of increased diffusional kurtosis in human brain following recent cerebral infarction. NMR Biomed 24, 452–457. 10.1002/nbm.1610 [PubMed: 20960579]

Jensen JH, Helpern JA, Ramani A, Lu H, Kaczynski K, 2005 Diffusional kurtosis imaging: the quantification of non-gaussian water diffusion by means of magnetic resonance imaging. Magn. Reson. Med 53, 1432–1440. 10.1002/mrm.20508 [PubMed: 15906300]

Jones DK, Knosche TR, Turner R, 2013 White matter integrity, fiber count, and other fallacies: the do's and don'ts of diffusion MRI. NeuroImage 73, 239–254. 10.1016/j.neuroimage.2012.06.081 [PubMed: 22846632]

Jones DK, Leemans A, 2011 Diffusion tensor imaging. Methods Mol. Biol. Clifton NJ 711, 127–144. 10.1007/978-1-61737-992-5_6

Kamagata K, Tomiyama H, Motoi Y, Kano M, Abe O, Ito K, Shimoji K, Suzuki M, Hori M, Nakanishi A, Kuwatsuru R, Sasai K, Aoki S, Hattori N, 2013 Diffusional kurtosis imaging of cingulate fibers in Parkinson disease: comparison with conventional diffusion tensor imaging. Magn. Reson. Imaging 31, 1501–1506. 10.1016/j.mri.2013.06.009 [PubMed: 23895870]

Katz J, d'Albis M-A, Boisgontier J, Poupon C, Mangin J-F, Guevara P, Duclap D, Hamdani N, Petit J, Monnet D, Le Corvoisier P, Leboyer M, Delorme R, Houenou J, 2016 Similar white matter but opposite grey matter changes in schizophrenia and high-functioning autism. Acta Psychiatr. Scand 134, 31–39. 10.1111/acps.12579 [PubMed: 27105136]

Kelly S, Jahanshad N, Zalesky A, Kochunov P, Agartz I, Alloza C, Andreassen OA, Arango C, Banaj N, Bouix S, Bousman CA, Brouwer RM, Bruggemann J, Bustillo J, Cahn W, Calhoun V, Cannon D, Carr V, Catts S, Chen J, Chen J-X, Chen X, Chiapponi C, Cho KK, Ciullo V, Corvin AS, Crespo-Facorro B, Cropley V, De Rossi P, Diaz-Caneja CM, Dickie EW, Ehrlich S, Fan F-M, Faskowitz J, Fatouros-Bergman H, Flyckt L, Ford JM, Fouche J-P, Fukunaga M, Gill M, Glahn DC, Gollub R, Goudzwaard ED, Guo H, Gur RE, Gur RC, Gurholt TP, Hashimoto R, Hatton SN, Henskens FA, Hibar DP, Hickie IB, Hong LE, Horacek J, Howells FM, Hulshoff Pol HE, Hyde CL, Isaev D, Jablensky A, Jansen PR, Janssen J, Jonsson EG, Jung LA, Kahn RS, Kikinis Z, Liu K, Klauser P, Knochel C, Kubicki M, Lagopoulos J, Langen C, Lawrie S, Lenroot RK, Lim KO, Lopez-Jaramillo C, Lyall A, Magnotta V, Mandl RCW, Mathalon DH, McCarley RW, McCarthy-Jones S, McDonald C, McEwen S, McIntosh A, Melicher T, Mesholam-Gately RI, Michie PT, Mowry B, Mueller BA, Newell DT, O'Donnell P, Oertel-Knochel V, Oestreich L, Paciga SA, Pantelis C, Pasternak O, Pearlson G, Pellicano GR, Pereira A, Pineda Zapata J, Piras F, Potkin SG, Preda A, Rasser PE, Roalf DR, Roiz R, Roos A, Rotenberg D, Satterthwaite TD, Savadjiev P, Schall U, Scott RJ, Seal ML, Seidman LJ, Shannon Weickert C, Whelan CD, Shenton ME, Kwon JS, Spalletta G, Spaniel F, Sprooten E, Stablein M, Stein DJ, Sundram S, Tan Y, Tan S, Tang S, Temmingh HS, Westlye LT, Tonnesen S, Tordesillas-Gutierrez D, Doan NT, Vaidya J, van Haren NEM, Vargas CD, Vecchio D, Velakoulis D, Voineskos A, Voyvodic JQ, Wang Z, Wan P, Wei D, Weickert TW, Whalley H, White T, Whitford TJ, Wojcik JD, Xiang H, Xie Z, Yamamori H, Yang F, Yao N, Zhang G, Zhao J, van Erp TGM, Turner J, Thompson PM, Donohoe G, 2017 Widespread white matter microstructural differences in schizophrenia across 4322 individuals: results from the ENIGMA Schizophrenia DTI Working Group. Mol. Psychiatry 10.1038/mp. 2017.170

Kennedy SH, 2008 Core symptoms of major depressive disorder: relevance to diagnosis and treatment. Dialogues Clin. Neurosci 10, 271–277. [PubMed: 18979940]

Kochunov P, Chiappelli J, Hong LE, 2013 Permeability-diffusivity modeling vs. fractional anisotropy on white matter integrity assessment and application in schizophrenia. NeuroImage Clin 3, 18–26. 10.1016/j.nicl.2013.06.019 [PubMed: 24179845]

Kochunov P, Chiappelli J, Wright SN, Rowland LM, Patel B, Wijtenburg SA, Nugent K, McMahon RP, Carpenter WT, Muellerklein F, Sampath H, Hong LE, 2014 Multimodal white matter imaging to investigate reduced fractional anisotropy and its age-related decline in schizophrenia. Psychiatry Res 223, 148–156. 10.1016/j.pscychresns.2014.05.004 [PubMed: 24909602]

Kochunov P, Jahanshad N, Marcus D, Winkler A, Sprooten E, Nichols TE, Wright SN, Hong LE, Patel B, Behrens T, Jbabdi S, Andersson J, Lenglet C, Yacoub E, Moeller S, Auerbach E, Ugurbil K, Sotiropoulos SN, Brouwer RM, Landman B, Lemaitre H, den Braber A, Zwiers MP, Ritchie S, van Hulzen K, Almasy L, Curran J, deZubicaray GI, Duggirala R, Fox P, Martin NG, McMahon KL, Mitchell B, Olvera RL, Peterson C, Starr J, Sussmann J, Wardlaw J, Wright M, Boomsma DI,

Kahn R, de Geus EJC, Williamson DE, Hariri A, van 't Ent D, Bastin ME, McIntosh A, Deary IJ, Hulshoff Pol HE, Blangero J, Thompson PM, Glahn DC, Van Essen DC, 2015 Heritability of fractional anisotropy in human white matter: a comparison of Human Connectome Project and ENIGMA-DTI data. NeuroImage 111, 300–311. 10.1016/j.neuroimage.2015.02.050 [PubMed: 25747917]

Kochunov P, Rowland LM, Fieremans E, Veraart J, Jahanshad N, Eskandar G, Du X, Muellerklein F, Savransky A, Shukla D, Sampath H, Thompson PM, Hong LE, 2016 Diffusion-weighted imaging uncovers likely sources of processing-speed deficits in schizophrenia. Proc. Natl. Acad. Sci. U.S.A 113, 13504–13509. 10.1073/pnas.1608246113 [PubMed: 27834215]

Kubicki M, McCarley R, Westin C-F, Park H-J, Maier S, Kikinis R, Jolesz FA, Shenton ME, 2007 A review of diffusion tensor imaging studies in schizophrenia. J. Psychiatr. Res 41, 15–30. 10.1016/j.jpsychires.2005.05.005 [PubMed: 16023676]

Kubicki M, Shenton ME, 2014 Diffusion Tensor Imaging findings and their implications in schizophrenia. Curr. Opin. Psychiatry 27, 179–184. 10.1097/YCO.0000000000000053 [PubMed: 24613986]

Lampinen B, Szczepankiewicz F, Mårtensson J, van Westen D, Sundgren PC, Nilsson M, 2017 Neurite density imaging versus imaging of microscopic anisotropy in diffusion MRI: A model comparison using spherical tensor encoding. NeuroImage 147, 517–531. 10.1016/j.neuroimage.2016.11.053 [PubMed: 27903438]

Lasi S, Nilsson M, Lätt J, Ståhlberg F, Topgaard D, 2011 Apparent exchange rate mapping with diffusion MRI. Magn. Reson. Med 66, 356–365. 10.1002/mrm.22782 [PubMed: 21446037]

Le Bihan D, Turner R, MacFall JR, 1989 Effects of intravoxel incoherent motions (IVIM) in steady-state free precession (SSFP) imaging: application to molecular diffusion imaging. Magn. Reson. Med 10, 324–337. [PubMed: 2733589]

Lepage M, Bodnar M, Bowie CR, 2014 Neurocognition: Clinical and Functional Outcomes in Schizophrenia. Can. J. Psychiatry 59, 5–12. 10.1177/070674371405900103 [PubMed: 24444318]

Liao Y, Huang X, Wu Q, Yang C, Kuang W, Du M, Lui S, Yue Q, Chan RCK, Kemp GJ, Gong Q, 2013 Is depression a disconnection syndrome? Metaanalysis of diffusion tensor imaging studies in patients with MDD. J. Psychiatry Neurosci. JPN 38, 49–56. 10.1503/jpn.110180 [PubMed: 22691300]

Linden DEJ, 2012 The Challenges and Promise of Neuroimaging in Psychiatry. Neuron 73, 8–22. 10.1016/j.neuron.2011.12.014 [PubMed: 22243743]

Lyall AE, Pasternak O, Robinson DG, Newell D, Trampush JW, Gallego JA, Fava M, Malhotra AK, Karlsgodt KH, Kubicki M, Szeszko PR, 2017 Greater extracellular free-water in first episode psychosis predicts better neurocognitive functioning. Mol. Psychiatry 10.1038/mp.2017.43

MacQueen GM, 2010 Will there be a role for neuroimaging in clinical psychiatry? J. Psychiatry Neurosci. JPN 35, 291–293. 10.1503/jpn.100129 [PubMed: 20731963]

Mandl RCW, Pasternak O, Cahn W, Kubicki M, Kahn RS, Shenton ME, Hulshoff Pol HE, 2015 Comparing free water imaging and magnetization transfer measurements in schizophrenia. Schizophr. Res 161, 126–132. 10.1016/j.schres.2014.09.046 [PubMed: 25454797]

Matthews PM, Roncaroli F, Waldman A, Sormani MP, Stefano ND, Giovannoni G, Reynolds R, 2016 A practical review of the neuropathology and neuroimaging of multiple sclerosis. Pract. Neurol 16, 279–287. 10.1136/practneurol-2016-001381 [PubMed: 27009310]

Mendelsohn A, Strous RD, Bleich M, Assaf Y, Hendler T, 2006 Regional axonal abnormalities in first episode schizophrenia: Preliminary evidence based on high b-value diffusion-weighted imaging. Psychiatry Res. Neuroimaging 146, 223–229. 10.1016/j.pscychresns.2005.12.010

Metzler-Baddeley C, O'Sullivan MJ, Bells S, Pasternak O, Jones DK, 2012 How and how not to correct for CSF-contamination in diffusion MRI. NeuroImage 59, 1394–1403. 10.1016/j.neuroimage.2011.08.043 [PubMed: 21924365]

Michailovich O, Rathi Y, Dolui S, 2011 Spatially regularized compressed sensing for high angular resolution diffusion imaging. IEEE Trans. Med. Imaging 30, 1100–1115. 10.1109/TMI.2011.2142189 [PubMed: 21536524]

Mirzaalian H, Ning L, Savadjiev P, Pasternak O, Bouix S, Michailovich O, Grant G, Marx CE, Morey RA, Flashman LA, George MS, McAllister TW, Andaluz N, Shutter L, Coimbra R, Zafonte RD,

Coleman MJ, Kubicki M, Westin CF, Stein MB, Shenton ME, Rathi Y, 2016 Inter-site and interscanner diffusion MRI data harmonization. NeuroImage 135, 311–323. 10.1016/j.neuroimage. 2016.04.041 [PubMed: 27138209]

Mori S, Zhang J, 2006 Principles of diffusion tensor imaging and its applications to basic neuroscience research. Neuron 51, 527–539. 10.1016/j.neuron.2006.08.012 [PubMed: 16950152]

Mulders PC, van Eijndhoven PF, Schene AH, Beckmann CF, Tendolkar I, 2015 Resting-state functional connectivity in major depressive disorder: A review. Neurosci. Biobehav. Rev 56, 330–344. 10.1016/j.neubiorev.2015.07.014 [PubMed: 26234819]

Mulkern RV, Gudbjartsson H, Westin CF, Zengingonul HP, Gartner W, Guttmann CR, Robertson RL, Kyriakos W, Schwartz R, Holtzman D, Jolesz FA, Maier SE, 1999 Multi-component apparent diffusion coefficients in human brain. NMR Biomed 12, 51–62. [PubMed: 10195330]

Murphy ML, Frodl T, 2011 Meta-analysis of diffusion tensor imaging studies shows altered fractional anisotropy occurring in distinct brain areas in association with depression. Biol. Mood Anxiety Disord 1, 3 10.1186/2045-5380-1-3 [PubMed: 22738088]

Narita H, Tha KK, Hashimoto N, Hamaguchi H, Nakagawa S, Shirato H, Kusumi I, 2016 Mean kurtosis alterations of cerebral white matter in patients with schizophrenia revealed by diffusion kurtosis imaging. Prog. Neuropsychopharmacol. Biol. Psychiatry 71, 169–175. 10.1016/j.pnpbp. 2016.07.011 [PubMed: 27495358]

National Collaborating Centre for Mental Health UK, 2006 BIPOLAR DISORDER AND ITS DIAGNOSIS, 4th ed. British Psychological Society.

Nazeri A, Mulsant BH, Rajji TK, Levesque ML, Pipitone J, Stefanik L, Shahab S, Roostaei T, Wheeler AL, Chavez S, Voineskos AN, 2016 Gray Matter Neuritic Microstructure Deficits in Schizophrenia and Bipolar Disorder. Biol. Psychiatry 10.1016/j.biopsych.2016.12.005

Nilsson M, van Westen D, Stahlberg F, Sundgren PC, Latt J, 2013 The role of tissue microstructure and water exchange in biophysical modelling of diffusion in white matter. Magma N. Y. N 26, 345–370. 10.1007/s10334-013-0371-x

Ning L, Setsompop K, Michailovich O, Makris N, Shenton ME, Westin C-F, Rathi Y, 2016 A joint compressed-sensing and super-resolution approach for very high-resolution diffusion imaging. NeuroImage 125, 386–400. 10.1016/j.neuroimage.2015.10.061 [PubMed: 26505296]

Nortje G, Stein DJ, Radua J, Mataix-Cols D, Horn N, 2013 Systematic review and voxel-based meta-analysis of diffusion tensor imaging studies in bipolar disorder. J. Affect. Disord 150, 192–200. 10.1016/j.jad.2013.05.034 [PubMed: 23810479]

Novikov DS, Fieremans E, Jensen JH, Helpern JA, 2011 Random walk with barriers. Nat. Phys 7, 508–514. 10.1038/nphys1936 [PubMed: 21686083]

O'Donnell LJ, Pasternak O, 2015 Does diffusion MRI tell us anything about the white matter? An overview of methods and pitfalls. Schizophr. Res 161, 133–141. 10.1016/j.schres.2014.09.007 [PubMed: 25278106]

Oestreich LKL, Lyall AE, Pasternak O, Kikinis Z, Newell DT, Savadjiev P, Bouix S, Shenton ME, Kubicki M, Australian Schizophrenia Research Bank, Whitford TJ, McCarthy-Jones S, 2017 Characterizing white matter changes in chronic schizophrenia: A free-water imaging multi-site study. Schizophr. Res 10.1016/j.schres.2017.02.006

Oestreich LKL, Pasternak O, Shenton ME, Kubicki M, Gong X, Australian Schizophrenia Research Bank, McCarthy-Jones S, Whitford TJ, 2016 Abnormal white matter microstructure and increased extracellular freewater in the cingulum bundle associated with delusions in chronic schizophrenia. NeuroImage Clin 12, 405–414. 10.1016/j.nicl.2016.08.004 [PubMed: 27622137]

Pasternak O, Kubicki M, Shenton ME, 2016 In vivo imaging of neuroinflammation in schizophrenia. Schizophr. Res 173, 200–212. 10.1016/j.schres.2015.05.034 [PubMed: 26048294]

Pasternak O, Sochen N, Gur Y, Intrator N, Assaf Y, 2009 Free water elimination and mapping from diffusion MRI. Magn. Reson. Med 62, 717–730. 10.1002/mrm.22055 [PubMed: 19623619]

Pasternak O, Westin C-F, Bouix S, Seidman LJ, Goldstein JM, Woo T-UW, Petryshen TL, Mesholam-Gately RI, McCarley RW, Kikinis R, Shenton ME, Kubicki M, 2012 Excessive extracellular volume reveals a neurodegenerative pattern in schizophrenia onset. J. Neurosci. Off. J. Soc. Neurosci 32, 17365–17372. 10.1523/JNEUROSCI.2904-12.2012

Phillips ML, Swartz HA, 2014 A critical appraisal of neuroimaging studies of bipolar disorder: toward a new conceptualization of underlying neural circuitry and a road map for future research. Am. J. Psychiatry 171, 829–843. 10.1176/appi.ajp.2014.13081008 [PubMed: 24626773]

Pierpaoli C, Basser PJ, 1996 Toward a quantitative assessment of diffusion anisotropy. Magn. Reson. Med 36, 893–906. 10.1002/mrm.1910360612 [PubMed: 8946355]

Pierpaoli C, Jezzard P, Basser PJ, Barnett A, Di Chiro G, 1996 Diffusion tensor MR imaging of the human brain. Radiology 201, 637–648. 10.1148/radiology.201.3.8939209 [PubMed: 8939209]

Plum F, 1972 Prospects for research on schizophrenia. 3. Neurophysiology. Neuropathological findings. Neurosci. Res. Program Bull 10, 384–388. [PubMed: 4663816]

Popescu BFG, Lucchinetti CF, 2016 Chapter 9 - Neuropathology of Multiple Sclerosis, in: Minagar A (Ed.), Multiple Sclerosis Academic Press, San Diego, pp. 181–200. 10.1016/B978-0-12-800763-1.00009-9

Raab P, Hattingen E, Franz K, Zanella FE, Lanfermann H, 2010 Cerebral gliomas: diffusional kurtosis imaging analysis of microstructural differences. Radiology 254, 876–881. 10.1148/radiol.09090819 [PubMed: 20089718]

Rae CL, Davies G, Garfinkel SN, Gabel MC, Dowell NG, Cercignani M, Seth AK, Greenwood KE, Medford N, Critchley HD, 2017 Deficits in Neurite Density Underlie White Matter Structure Abnormalities in First episode Psychosis. Biol. Psychiatry, Risk Genes and the Emergence of Schizophrenia 82, 716–725. 10.1016/j.biopsych.2017.02.008

Ramani A, Jensen J, Szule K, Ali O, Hu C, Lu H, Brodie J, Helpern J, 2007 Assessment of abnormalities in the cerebral microstructure of schizophrenia patients - a diffusional kurtosis imaging study. Proc Intl Soc Mag Reson Med 15.

Rathi Y, Malcolm J, Michailovich O, Goldstein J, Seidman L, McCarley RW, Westin C-F, Shenton ME, 2010 Biomarkers for identifying first episode schizophrenia patients using diffusion weighted imaging. Med. Image Comput. Comput.-Assist. Interv. MICCAI Int. Conf. Med. Image Comput. Comput.-Assist. Interv 13, 657–665.

Rydhög AS, Szczepankiewicz F, Wirestam R, Ahlgren A, Westin C-F, Knutsson L, Pasternak O, 2017 Separating blood and water: Perfusion and free water elimination from diffusion MRI in the human brain. NeuroImage 156, 423–434. 10.1016/j.neuroimage.2017.04.023 [PubMed: 28412443]

Sarrazin S, Poupon C, Linke J, Wessa M, Phillips M, Delavest M, Versace A, Almeida J, Guevara P, Duclap D, Duchesnay E, Mangin J-F, Le Dudal K, Daban C, Hamdani N, D'Albis M-A, Leboyer M, Houenou J, 2014 A multicenter tractography study of deep white matter tracts in bipolar I disorder: psychotic features and interhemispheric disconnectivity. JAMA Psychiatry 71, 388–396. 10.1001/jamapsychiatry.2013.4513 [PubMed: 24522197]

Sato K, Kerever A, Kamagata K, Tsuruta K, Irie R, Tagawa K, Okazawa H, Arikawa-Hirasawa E, Nitta N, Aoki I, Aoki S, 2017 Understanding microstructure of the brain by comparison of neurite orientation dispersion and density imaging (NODDI) with transparent mouse brain. Acta Radiol. Open 6, 2058460117703816. 10.1177/2058460117703816

Savadjiev P, Whitford TJ, Hough ME, Clemm von Hohenberg C, Bouix S, Westin C-F, Shenton ME, Crow TJ, James AC, Kubicki M, 2014 Sexually dimorphic white matter geometry abnormalities in adolescent onset schizophrenia. Cereb. Cortex N. Y. N 1991 24, 1389–1396. 10.1093/cercor/bhs422

Scholz V, Houenou J, Kollmann B, Duclap D, Poupon C, Wessa M, 2016 Dysfunctional decision-making related to white matter alterations in bipolar I disorder. J. Affect. Disord 194, 72–79. 10.1016/j.jad.2015.12.019 [PubMed: 26803778]

Seal ML, Yucel M, Fornito A, Wood SJ, Harrison BJ, Walterfang M, Pell GS, Pantelis C, 2008 Abnormal white matter microstructure in schizophrenia: a voxelwise analysis of axial and radial diffusivity. Schizophr. Res 101, 106–110. 10.1016/j.schres.2007.12.489 [PubMed: 18262770]

Seroussi I, Grebenkov DS, Pasternak O, Sochen N, 2017 Microscopic interpretation and generalization of the Bloch-Torrey equation for diffusion magnetic resonance. J. Magn. Reson 277, 95–103. 10.1016/j.jmr.2017.01.018 [PubMed: 28242566]

Setsompop K, Feinberg DA, Polimeni JR, 2016 Rapid brain MRI acquisition techniques at ultra-high fields. NMR Biomed 29, 1198–1221. 10.1002/nbm.3478 [PubMed: 26835884]

Sexton CE, Mackay CE, Ebmeier KP, 2009 A systematic review of diffusion tensor imaging studies in affective disorders. Biol. Psychiatry 66, 814–823. 10.1016/j.biopsych.2009.05.024 [PubMed: 19615671]

Shen C-Y, Tyan Y-S, Kuo L-W, Wu CW, Weng J-C, 2015 Quantitative Evaluation of Rabbit Brain Injury after Cerebral Hemisphere Radiation Exposure Using Generalized q-Sampling Imaging. PloS One 10, e0133001 10.1371/journal.pone.0133001 [PubMed: 26168047]

Shenton ME, Dickey CC, Frumin M, McCarley RW, 2001 A review of MRI findings in schizophrenia. Schizophr. Res 49, 1–52. 10.1016/S0920-9964(01)00163-3

Shulman JM, De Jager PL, Feany MB, 2011 Parkinson's disease: genetics and pathogenesis. Annu. Rev. Pathol 6, 193–222. 10.1146/annurev-pathol-011110-130242 [PubMed: 21034221]

Song S-K, Sun S-W, Ramsbottom MJ, Chang C, Russell J, Cross AH, 2002 Dysmyelination Revealed through MRI as Increased Radial (but Unchanged Axial) Diffusion of Water. NeuroImage 17, 1429–1436. 10.1006/nimg.2002.1267 [PubMed: 12414282]

Souza-Queiroz J, Boisgontier J, Etain B, Poupon C, Duclap D, d'Albis M-A, Daban C, Hamdani N, Le Corvoisier P, Delavest M, Bellivier F, Guevara P, Leboyer M, Henry C, Houenou J, 2016 Childhood trauma and the limbic network: a multimodal MRI study in patients with bipolar disorder and controls. J. Affect. Disord 200, 159–164. 10.1016/j.jad.2016.04.038 [PubMed: 27136413]

Stanisz GJ, Szafer A, Wright GA, Henkelman RM, 1997 An analytical model of restricted diffusion in bovine optic nerve. Magn. Reson. Med 37, 103–111. [PubMed: 8978638]

Sukstanskii AL, Ackerman JJH, Yablonskiy DA, 2003 Effects of barrier-induced nuclear spin magnetization inhomogeneities on diffusion-attenuated MR signal. Magn. Reson. Med 50, 735–742. 10.1002/mrm.10586 [PubMed: 14523959]

Sukstanskii AL, Yablonskiy DA, Ackerman JJH, 2004 Effects of permeable boundaries on the diffusion-attenuated MR signal: insights from a onedimensional model. J. Magn. Reson 170, 56–66. 10.1016/j.jmr.2004.05.020 [PubMed: 15324758]

Syková E, Nicholson C, 2008 Diffusion in brain extracellular space. Physiol. Rev 88, 1277–1340. 10.1152/physrev.00027.2007 [PubMed: 18923183]

Tournier J-D, Mori S, Leemans A, 2011 Diffusion Tensor Imaging and Beyond. Magn. Reson. Med 65, 1532–1556. 10.1002/mrm.22924 [PubMed: 21469191]

Tseng C-EJ, Chien Y-L, Liu C-M, Wang H-LS, Hwu H-G, Tseng W-YI, 2015 Altered cortical structures and tract integrity of the mirror neuron system in association with symptoms of schizophrenia. Psychiatry Res 231, 286–291. 10.1016/j.pscychresns.2015.01.010 [PubMed: 25659475]

Tuch DS, 2004 Q-ball imaging. Magn. Reson. Med 52, 1358–1372. 10.1002/mrm.20279 [PubMed: 15562495]

Tuozzo C, Lyall AE, Pasternak O, James ACD, Crow TJ, Kubicki M, 2017 Patients with chronic bipolar disorder exhibit widespread increases in extracellular free water. Bipolar Disord 10.1111/bdi.12588

Uher R, Payne JL, Pavlova B, Perlis RH, 2014 Major depressive disorder in DSM- 5: implications for clinical practice and research of changes from DSM-IV. Depress. Anxiety 31, 459–471. 10.1002/da.22217 [PubMed: 24272961]

Umesh Rudrapatna S, Wieloch T, Beirup K, Ruscher K, Mol W, Yanev P, Leemans A, van der Toorn A, Dijkhuizen RM, 2014 Can diffusion kurtosis imaging improve the sensitivity and specificity of detecting microstructural alterations in brain tissue chronically after experimental stroke? Comparisons with diffusion tensor imaging and histology. NeuroImage 97, 363–373. 10.1016/j.neuroimage.2014.04.013 [PubMed: 24742916]

Vargas C, López-Jaramillo C, Vieta E, 2013 A systematic literature review of resting state network-- functional MRI in bipolar disorder. J. Affect. Disord 150, 727–735. 10.1016/j.jad.2013.05.083 [PubMed: 23830141]

Wang C, Ji F, Hong Z, Poh JS, Krishnan R, Lee J, Rekhi G, Keefe RSE, Adcock RA, Wood SJ, Fornito A, Pasternak O, Chee MWL, Zhou J, 2016 Disrupted salience network functional connectivity and white-matter microstructure in persons at risk for psychosis: findings from the LYRIKS study. Psychol. Med 46, 2771–2783. 10.1017/S0033291716001410 [PubMed: 27396386]

Wedeen VJ, Hagmann P, Tseng W-YI, Reese TG, Weisskoff RM, 2005 Mapping complex tissue architecture with diffusion spectrum magnetic resonance imaging. Magn. Reson. Med 54, 1377–1386. 10.1002/mrm.20642 [PubMed: 16247738]

Westin C-F, Knutsson H, Pasternak O, Szczepankiewicz F, Ozarslan E, van Westen D, Mattisson C, Bogren M, O'Donnell LJ, Kubicki M, Topgaard D, Nilsson M, 2016 Q-space trajectory imaging for multidimensional diffusion MRI of the human brain. NeuroImage 135, 345–362. 10.1016/j.neuroimage.2016.02.039 [PubMed: 26923372]

Weyandt L, Swentosky A, Gudmundsdottir BG, 2013 Neuroimaging and ADHD: fMRI, PET, DTI findings, and methodological limitations. Dev. Neuropsychol 38, 211–225. 10.1080/87565641.2013.783833 [PubMed: 23682662]

Wheeler AL, Voineskos AN, 2014 A review of structural neuroimaging in schizophrenia: from connectivity to connectomics. Front. Hum. Neurosci 8 10.3389/fnhum.2014.00653

Wu C-H, Hwang T-J, Chen P-J, Chou T-L, Hsu Y-C, Liu C-M, Wang H-L, Chen C-M, Hua M-S, Hwu H-G, Tseng W-YI, 2014 Reduced structural integrity and functional lateralization of the dorsal language pathway correlate with hallucinations in schizophrenia: a combined diffusion spectrum imaging and functional magnetic resonance imaging study. Psychiatry Res 224, 303–310. 10.1016/j.pscychresns.2014.08.010 [PubMed: 25241043]

Wu C-H, Hwang T-J, Chen Y-J, Hsu Y-C, Lo Y-C, Liu C-M, Hwu H-G, Liu C-C, Hsieh MH, Chien Y-L, Chen C-M, Isaac Tseng W-Y, 2015a Primary and secondary alterations of white matter connectivity in schizophrenia: A study on first episode and chronic patients using whole-brain tractography-based analysis. Schizophr. Res 169, 54–61. 10.1016/j.schres.2015.09.023 [PubMed: 26443482]

Wu C-H, Hwang T-J, Chen Y-J, Hsu Y-C, Lo Y-C, Liu C-M, Hwu H-G, Liu C-C, Hsieh MH, Chien YL, Chen C-M, Tseng W-YI, 2015b Altered integrity of the right arcuate fasciculus as a trait marker of schizophrenia: a sibling study using tractography-based analysis of the whole brain. Hum. Brain Mapp 36, 1065–1076. 10.1002/hbm.22686 [PubMed: 25366810]

Zhang H, Schneider T, Wheeler-Kingshott CA, Alexander DC, 2012 NODDI: practical in vivo neurite orientation dispersion and density imaging of the human brain. NeuroImage 61, 1000–1016. 10.1016/j.neuroimage.2012.03.072 [PubMed: 22484410]

Zhao L, Wang Y, Jia Y, Zhong S, Sun Y, Zhou Z, Zhang Z, Huang L, 2016 Cerebellar microstructural abnormalities in bipolar depression and unipolar depression: A diffusion kurtosis and perfusion imaging study. J. Affect. Disord 195, 21–31. 10.1016/j.jad.2016.01.042 [PubMed: 26852094]

Zhu J, Zhuo C, Liu F, Xu L, Yu C, 2016 Neural substrates underlying delusions in schizophrenia. Sci. Rep 6, 33857 10.1038/srep33857 [PubMed: 27651212]

Zhu J, Zhuo C, Qin W, Wang D, Ma X, Zhou Y, Yu C, 2015 Performances of diffusion kurtosis imaging and diffusion tensor imaging in detecting white matter abnormality in schizophrenia. NeuroImage Clin 7, 170–176. 10.1016/j.nicl.2014.12.008 [PubMed: 25610778]

Zhuo J, Xu S, Proctor JL, Mullins RJ, Simon JZ, Fiskum G, Gullapalli RP, 2012 Diffusion kurtosis as an in vivo imaging marker for reactive astrogliosis in traumatic brain injury. NeuroImage 59, 467–477. 10.1016/j.neuroimage.2011.07.050 [PubMed: 21835250]
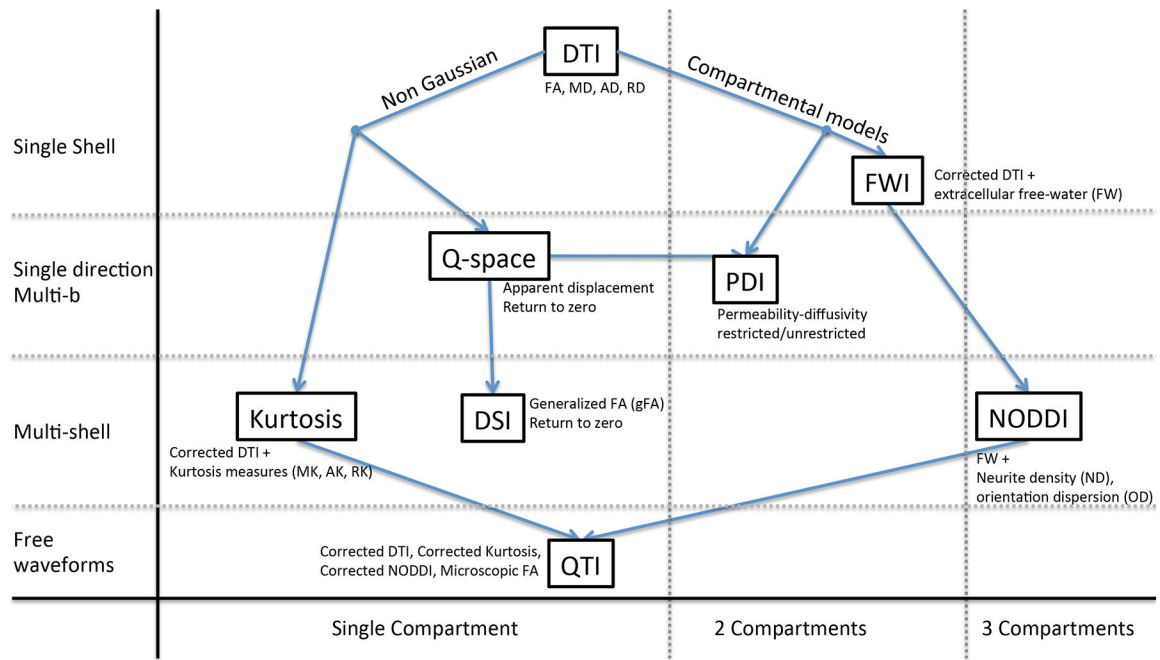
Figure 1: An overview of the advanced diffusion MRI methods examined in this article.
The methods are either model based (Compartmental models) or non-model based (Non Gaussian), with the later methods focusing on measures of deviation from a Gaussian distribution. Methods are ordered vertically by increased acquisition complexity (single shell, single direction multi-b, multi-shell and free-waveform), and horizontally by increased model complexity (1, 2 or 3 compartments). DTI = diffusion tensor imaging; FWI = Free-water imaging; PDI = Permeability-diffusivity imaging; DSI = Diffusion spectrum imaging; NODDI = Neurite orientation dispersion and density imaging; QTI = q-space trajectory imaging.

Parallel fibers:

Axon

Water molecules preferentially move parallel to the axons.

FA: High

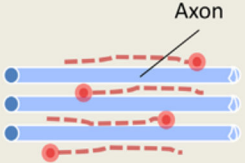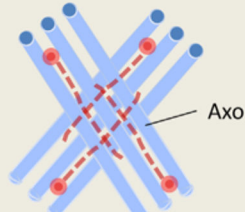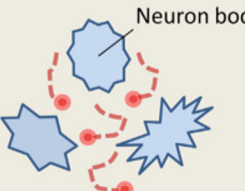**MD**: Low-medium

PTO: High

GFA: High

Fiber crossings:

Axon

Water molecules preferentially move parallel to the axons. There are two preferential axes of diffusion (i.e., the two tracts).

FA: Low-medium [I]

MD: Medium

PTO: High

GFA: Medium-high [I,II]

Gray matter:

Neuron body

Neuronal cells prevent water molecules from moving freely. Molecular mobility is "quasi-equal" in all directions.

FA: Low

MD: Medium

PTO: Medium

GFA: Low

CSF:

Water molecules diffuse freely without colliding with obstacles. Molecular mobility is equal in all directions.

FA: Null [III]

MD: High

PTO: Low

GFA: Null [III]

[I] Depending on the inter-fiber angle of the crossing and/or the degree of divergence and the relative contribution of each fiber bundle to the observed signal.
[II] It depends on the experimental diffusion MRI sequence and in particular on the b-value used. For higher b-values, higher GFA values are obtained.
[III] Imaging artifacts due to subject motion and the experimental MRI noise can result in low rather than null values.

Figure 2: Generalized fractional anisotropy (gFA).
(Canales-Rodríguez et al., 2014) proposed that the combination of gFA, probability of return to origin (PTO), FA and MD measures may best capture the diversity of microstructural environments in the brain, including regions of coherent parallel fibers, crossing fibers, gray matter, and cerebrospinal fluid (CSF). (Figure replicated from (Canales-Rodríguez et al., 2014) with permission).
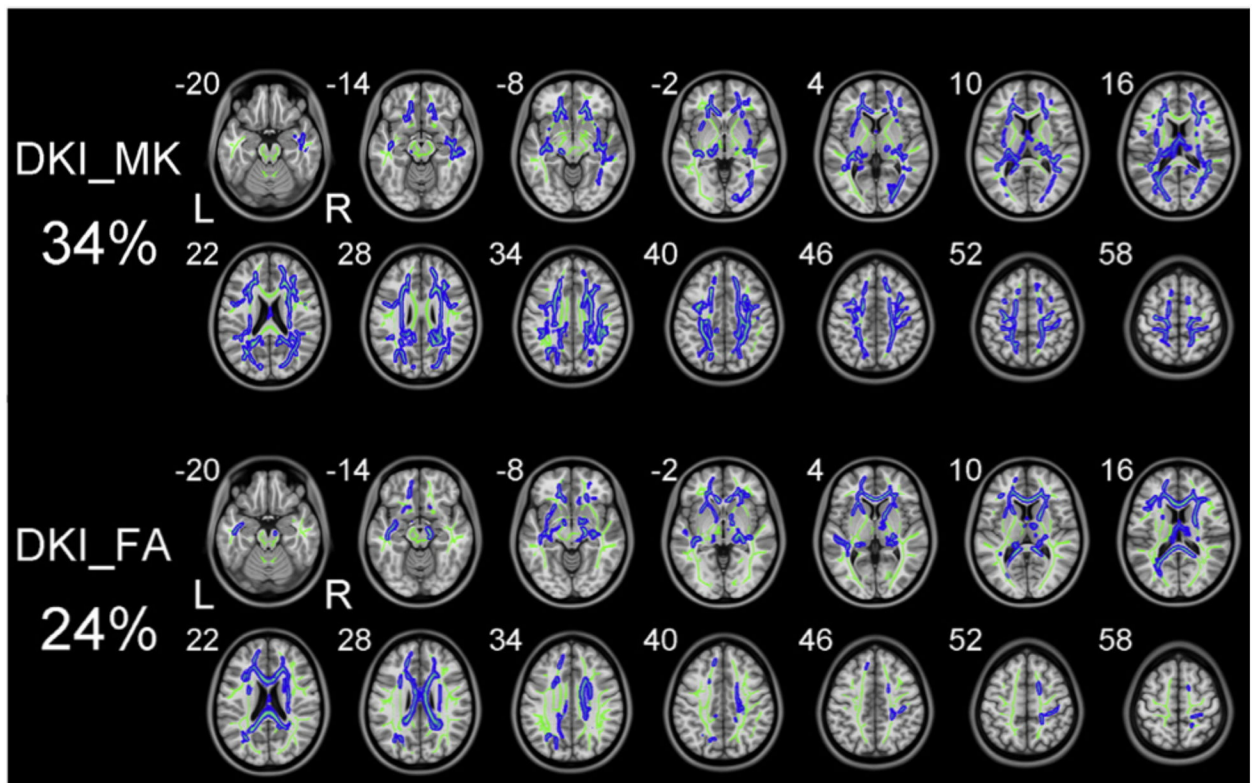
Figure 3: Direct comparison of DKI and DTI parameters.
Zhu et al. (2015) directly compared MK and FA measures derived from the DKI model. Despite much overlap between MK and FA, the FA measure identified abnormalities in ordered white matter bundles that MK could not identify (e.g., corpus callosum in z-coordinate 28). On the other hand, MK identified abnormalities in complex white matter structures that include crossing fibers, while FA did not identify abnormalities in those regions. (Figure modified from Zhu et al. (2015) with permission).
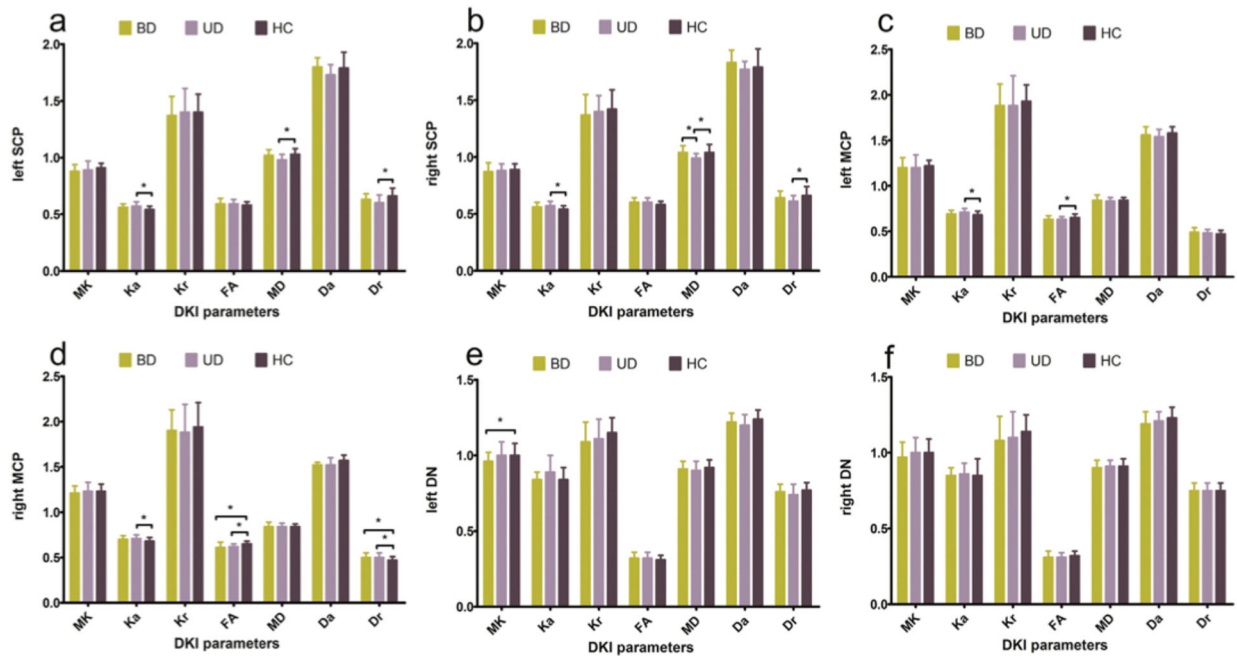
The units for MD, Da and Dr are all μm²/ms; MK, Ka, Kr and FA are dimensionless parameters.

Figure 4: Comparison of DKI and DTI parameters across disorders.
Zhao et al. (2016) compared DKI and DTI parameters between subjects with bipolar disorder, unipolar depression and healthy controls in the white matter of the superior and middle cerebellar peduncles (SCP and MCP), and in the dentate nuclei (DN). DKI (but not DTI) identified abnormalities in the DN. DTI and DKI identified the same abnormalities in the left SCP and left MCP. In the right MCP, both DTI and DKI identified a difference between unipolar depression patients and controls, however, DTI measures also identified a difference between bipolar disorder patients and controls. (Figure replicated from Zhao et al. (2016) with permission).
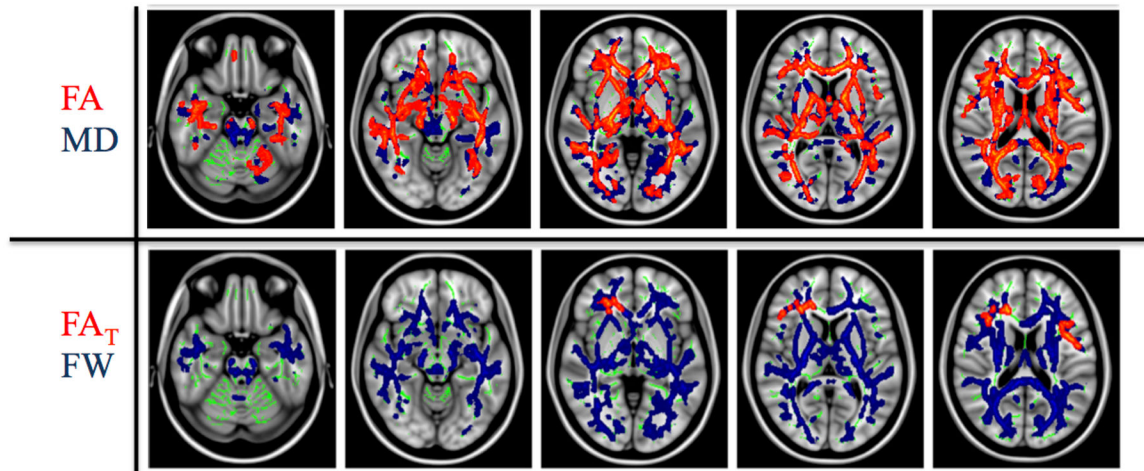
Figure 5: Comparison of Free-water imaging and DTI measures.
(Pasternak et al., 2012) compared free-water and DTI measures between first episode schizophrenia patients and controls. The widespread FA decreases (top, red) were explained mostly by increased fractional volume of extracellular free-water (FW) (bottom, blue). Following free-water correction the corrected tissue anisotropy (FA_T) was reduced only in a limited area in the frontal lobe. (Figure modified from Pasternak et al. (2012) with permission).

DTI model

$$S(b) = S_0 \cdot e^{-\vec{b} \cdot \bar{\bar{D}}}$$

$$FA = \frac{(D_{II} - D_\perp)}{\sqrt{D_{II}^2 + 2D_\perp^2}}$$

Permeability-diffusivity model

$$S(b) = S_0 \cdot (M_u \cdot e^{-b \cdot D_u} + (1 - M_u) \cdot e^{-b \cdot D_r}))$$

$$PDI = \frac{D_r}{D_u}$$
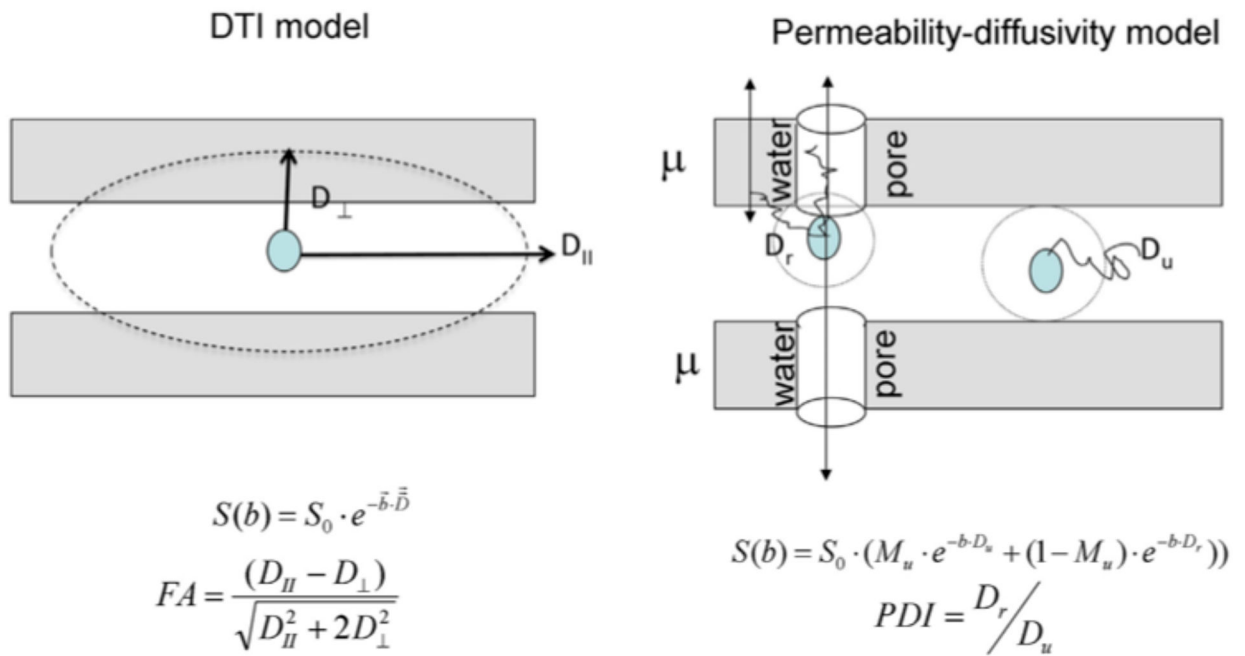
Figure 6: Permeability diffusivity imaging (PDI).
This illustration explains the PDI parameters in comparison to the DTI model. While DTI has one compartment, PDI assumes two compartments: a restricted compartment, next to membranes, and an unrestricted compartment, away from membranes. The ratio between the diffusivities of the two compartments defines the permeability diffusivity index, which is purported to reflect alterations in water channels embedded in the plasma membrane. (Replicated from Kochunov et al. (2013) with permission).
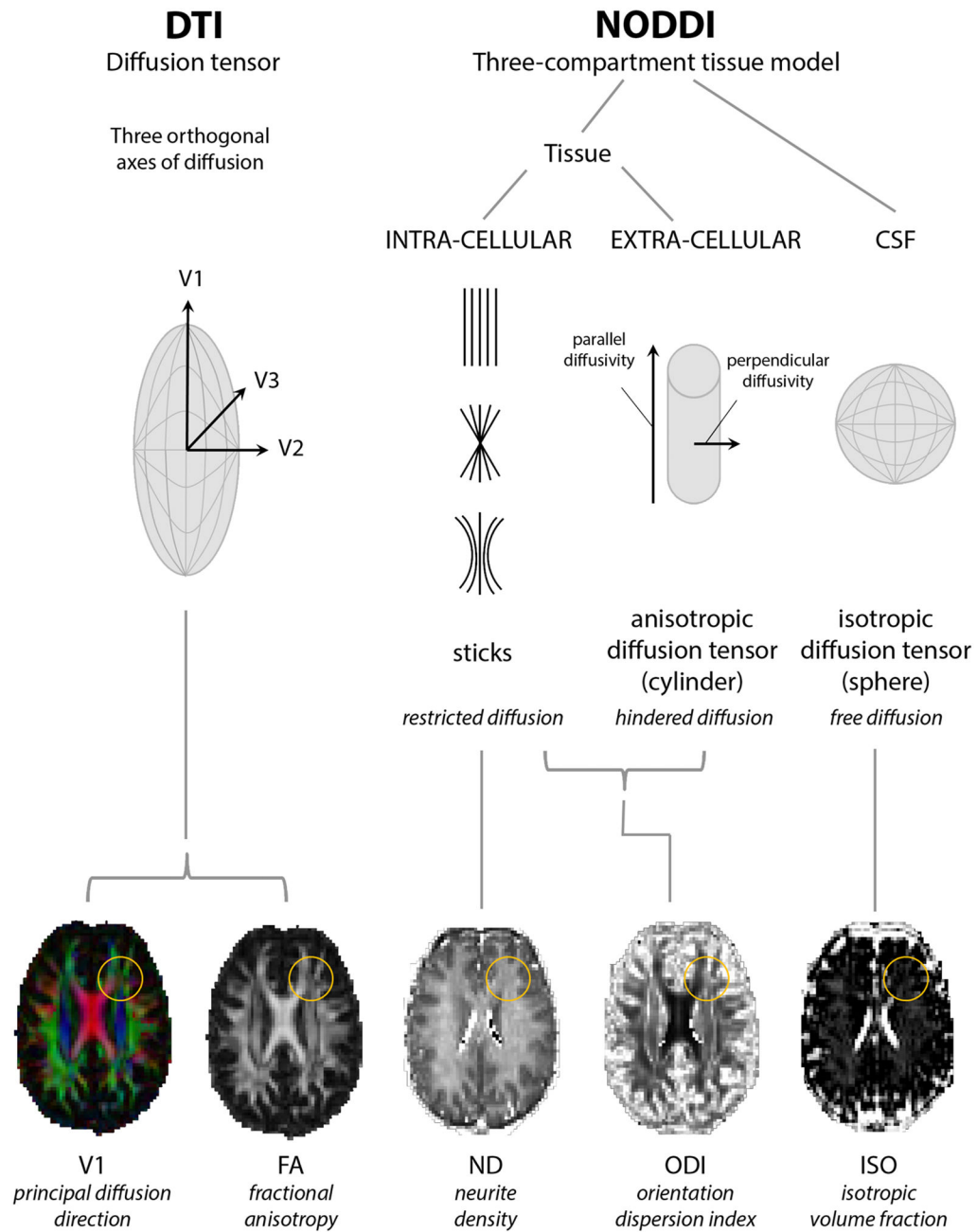
Figure 7: Neurite orientation dispersion and density imaging (NODDI).
NODDI has three compartments, intra-cellular, extra-cellular and CSF (free-water) compartments. The fractional volume of the isotropic compartment (ISO), the orientation dispersion index (ODI) and the neurite density (ND) are estimated from NODDI. (Figure replicated from Rae et al. (2017) with permission).
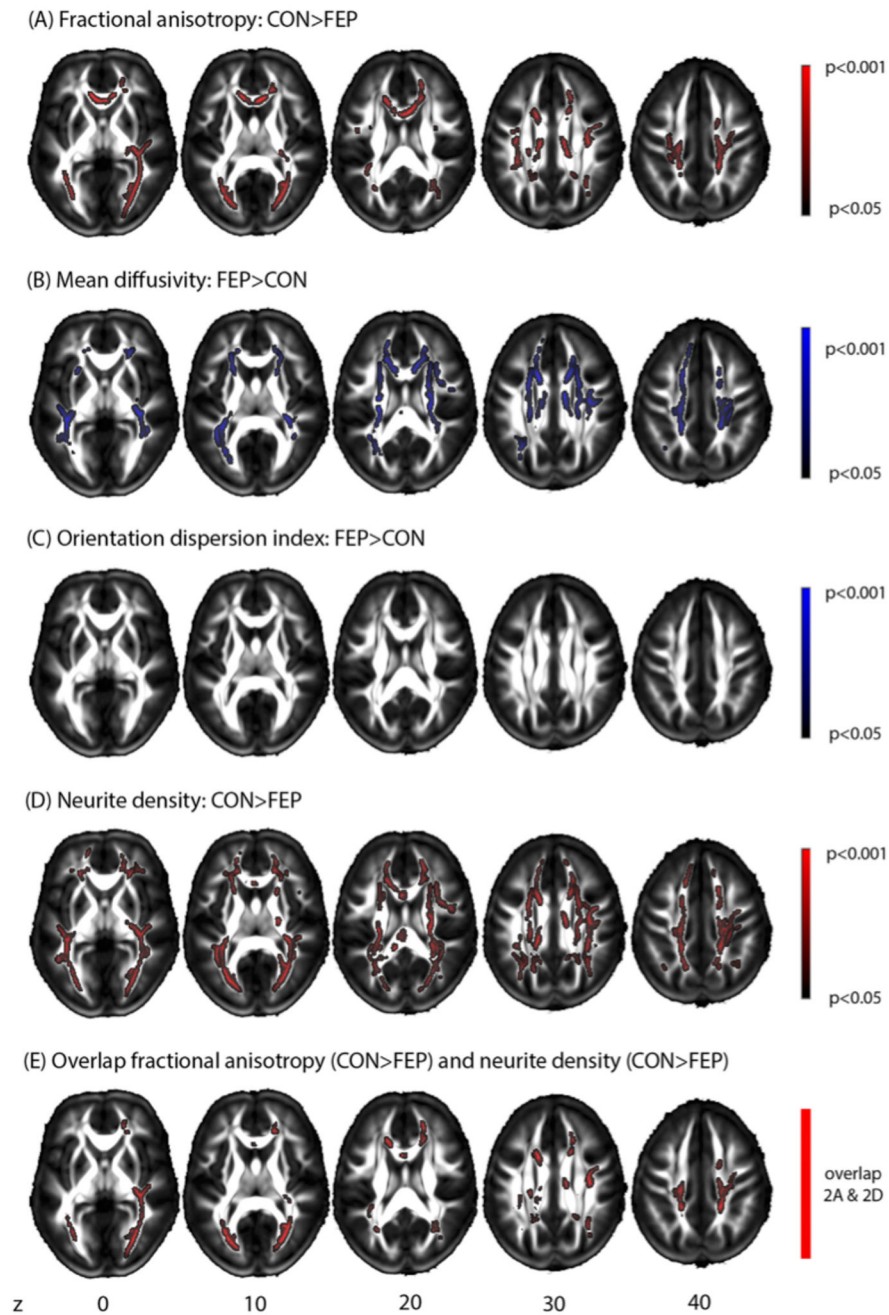
Figure 8: Comparison of NODDI and DTI measures.
Rae et al. (2017) compared DTI and NODDI measures in first episode schizophrenia patients (FEP) and controls (CON). Differences in FA predominantly co-localized with regions of reduced neurite density index (NDI), rather than with the orientation dispersion index (ODI).

Synthetic tensor distributions

Sticks - one size   Spheres - multiple sizes   Ellipsoids - multiple sizes

Corresponding DTD models: average and covariances

$\langle \mathbf{D} \rangle$ $\mathbb{C}$ $\langle \mathbf{D} \rangle$ $\mathbb{C}$ $\langle \mathbf{D} \rangle$ $\mathbb{C}$

MD $= 0.80$
$V_{\text{MD}} = 0.00$
$V_{\text{shear}} = 0.52$

MD $= 0.80$
$V_{\text{MD}} = 0.52$
$V_{\text{shear}} = 0.00$

MD $= 0.80$
$V_{\text{MD}} = 0.42$
$V_{\text{shear}} = 0.10$
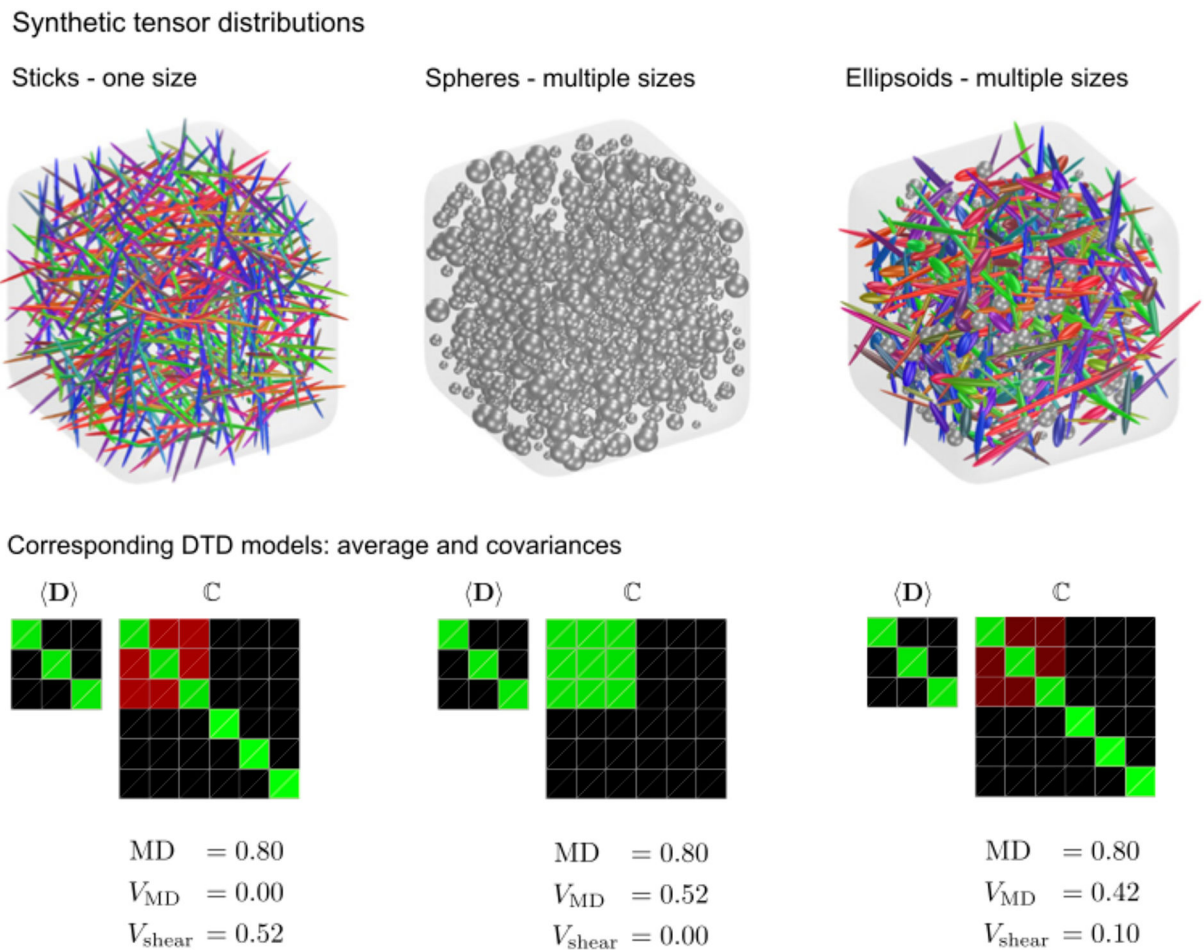
Figure 9: Q-space trajectory imaging (QTI).
Using a combination of continuous gradient pulses, QTI estimates a 4$^{\text{th}}$ order tensor, from which scalar values can be estimated. These parameters reflect features of the diffusion tensor distribution (DTD) such as size variability - V_{MD}, and shape variability – V_{shear}. The figure (replicated from Westin et al., 2016 with permission) shows three theoretical distributions that are macroscopically isotropic and thus indistinguishable using DTI parameters (or any other approach based on conventional pulsed gradients), but that can be separated based on their V_{MD} and V_{shear} values. In these graphical representations, green is positive, black is zero, and red is negative.

Summary table of schizophrenia studies

Study	Measure	Analysis method	Sample	Results
Mendelsohn et al (2006)	QSI and DTI	Histogram and ROI analysis	9 first-episode schizophrenia patients (6M/3F; 26 years (6)) 5 healthy controls (2M/3F; 29 years (3))	Lower return-to-zero probability and higher apparent displacement in white matter tissue for patients Anterior-prefrontal fibres had more pronounced differences compared to posterior-temporal fibers - this correlated with severity of positive and negative symptoms White matter differences more prominent in patients diagnosed as markedly ill Mildly ill patients did not differ from controls. Conventional DTI measures were not sensitive to early WM changes in this sample
Huang et al. (2010)	gFA	Tract-based	12 schizophrenia patients (5M, 7F; 26.92 years (7.35))	Negative correlation between functional connectivity and gFA of the right inferior parietal lobe and left posterior cingulate gyrus/precuneus of the default mode network.
Huang et al. (2011)	gFA	Tract-based	11 schizophrenia patients (4F, 7M; 34.55 years (7.26))	Negative correlation for gene dosage of candidate vulnerability genes and gFA tracts between the posterior cingulate gyrus and precuneus of the default mode network
Wu et al. (2014)	gFA	Tract-based	18 schizophrenia patients (8M, 10F; 30.77 years (6.14)) 18 HC (8M/10F; 29.61 years (6.69))	Lower gFA in left ventral, right ventral and right dorsal tracts of patients. Positive correlation between gFA of the right dorsal pathway and the functional lateralization of the dorsal pathway in patients. Negative correlation between gFA of right dorsal pathway and scores of delusion/hallucination symptoms.
Wu et al. (2015)	gFA	Tract-based	31 schizophrenia patients (17 M/14 F; 33.90 years (8.09)) 31 unaffected siblings (18 M/13 F; 33.29 years (9.80)) 31 healthy controls (15 M/16 F; 31.26 years (9.14))	Significant differences in gFA between the groups in the arcuate, fornix, auditory tracts, optic radiation, the genu of the corpus callosum, dorsolateral prefrontal cortices, temporal poles, and hippocampi. Lower gFA of right arcuate fasciculus in both patients and unaffected siblings compared to controls gFA of right arcuate fasciculus exhibited a trend toward positive symptom scores
Wu et al. (2015)	gFA	Tract-based	31 chronic schizophrenia patients (12 M/19 F; 29.87 years (5.86)) 25 first-episode (15 M/10 F; 26.48 years (6.90)) 31 healthy controls (16 M/15 F; 28.70 years (8.07))	Significant differences between groups in the arcuate fasciculus, fornix, superior longitudinal fasciculus, and fibers of the corpus callosum to the bilateral dorsolateral prefrontal cortices (DLPFC), bilateral temporal poles, and bilateral hippocampi. Reduced connection of callosal fibers to bilateral DLPFC in chronic patients but not in first-episode patients. Reduced connection significantly predicted by duration of illness. Remaining six tracts showed significant differences across both first-episode and chronic patients but no association with clinical variables.
Tseng et al. (2015)	gFA	Tract-based	32 schizophrenia patients (17M/15F; 32.4(6.3)) 32 healthy controls (17M/15F; 32.0 (6.5))	Lower gFA for patients in fibers interconnecting bilateral pars opercularis

Study	Measure	Analysis method	Sample	Results
Griffa et al. (2015)	gFA	Network analysis	16 schizophrenia patients (42.0 years (10.1)) 15 healthy controls (41.1 years (9.6))	Identified a core of locations affected by schizophrenia. The average gFA of fibers connecting the core was reduced. MD of these fibres was increased.
Katz et al. (2016)	gFA	Tract-based	23 male high functioning autism (HFA) (26.65 years (6.51)) 24 male schizophrenia patients (31.21 (8.21)) 32 male healthy controls (29.84 years (9.21))	Lower gFA for both HFA and schizophrenia groups in the left fronto-occipital inferior fasciculus compared with controls.
Baumann et al. (2016)	gFA	Tract-based	42 early psychosis patients (28M/14 F; 25.0 years (5.4)) 42 healthy controls 29 M/13 F; 25.3 years (5.3))	Lower gFA for patients in the fornix as well as smaller volume in the hippocampus
Rathi et al. (2010)	gFA, gN, DTI (2-tensor)	Tract-based and histogram analysis	21 FE schizophrenia (17 M/4 F; 21.21 years (4.56)) 20 healthy controls (15 M/5 F; 22.47 years (3.48))	Higher classification accuracy for the gN parameter over the gFA parameter. Tensor based classifiers were better than spherical harmonics based classifiers.
Sarrazin (2014)	gFA	Tractography	118 bipolar patients (36.32 years (10.49); 47% male) 86 healthy controls (37.26 years (11.22); 41% male)	Compared with controls, BPI patients had significant reductions in mean gFA values along the body and the splenium of the corpus callosum, the left cingulum, and the anterior part of the left arcuate fasciculus. Patients with a history of psychotic features had a lower mean gFA than those without along the body of the corpus callosum.
Scholz (2016)	gFA	Whole-brain tractography	24 euthymic Bipolar-I patients (10 F/14 M; 44 years (10)) 24 healthy controls (10 F/14 M; 44 years (10))	Patients had lower gFA values than controls in the right cingulum. gFA values in the remaining tracts did not differ significantly between groups
Favre (2016)	gFA/MD	Tractography	24 euthymic bipolar patients split into two treatment groups: 12 Psychoeducation group (44.42 years (8.35); 66.67% female) 12 Psychosupport group (46 years (10.48); 33.33% female) 12 Control group (43.58 years (11.18); 66.67% female)	Reduced MD along the left uncinate fasciculus for patients after psychoeducation. Patients of the psychosupport group did not differ. No change in gFA of right and left uncinate fasciculus for both patient groups. No significant differences between BD and CTL at baseline for gFA or MD.
Souza-Queiroz (2016)	gFA	Whole-brain tractography	47 healthy controls (36.4 years (11.3); 22M/25F) 32 bipolar patients (35.8 years (11.2); 20M/12F)	Childhood trauma questionnaire total score was negatively correlated left UF gFA across the whole sample. Negative correlations of physical neglect with left UF gFA Most of the results were significant for bipolar patients.
Canales-Rodriguez (2014)	gFA	Whole-brain	40 BP1 patients (15 M/F20 F; 40.6 years (8.925) 40 controls (25 M/15 F; 40.4 years (9.3))	Significant FA reductions in the splenium of corpus callosum (CC) and right insula. Widespread pattern of increased MD in gray and white matter tissues including anterior cingulum, left insula, and subcortical nuclei in patients. Frontotemporal, subcortical, and cerebellar increases of gFA in patients.

Study	Measure	Analysis method	Sample	Results
Chen et al. (2016)	gFA, NQA, isotropic	Tract based	16 outpatients with MDD (3 M/13 F; 44.8 years (2.2)) 30 healthy controls (3 M/27 F; 45.0 years (1.88))	Decreased gFA and NQA (an alternative anisotropy measure) ware observed in the superior longitudinal fasciculus and increases in isotropic contribution in the frontal lobe among subjects with MDD.
Sarrazin (2013)	gFA	Tractography	118 bipolar patients (36.32 years (10.49); 47% male) 86 healthy controls (37.26 years (11.22); 41% male)	Patients with BD had lower gFA than controls along the corpus callosum (body and splenium), the left cingulum and the left arcuate fasciculus.
Ramani et al. (2007)	DKI and DTI	Voxel-based	10 schizophrenia patients (50.8 years (11.5)) 8 healthy controls (52.7 years (10.6))	Lower mean kurtosis (MK) and FA for patients in white matter of the prefrontal cortex MK more sensitive in discriminating between patients and controls, compared to FA and MD measures
Zhu et al. (2015)	DKI and DTI	TBSS	94 schizophrenia patients (38 F/56 M; 33.5 years (8.4)) 91 healthy controls. (46 F/45 M; 33.5 years (10.3))	DTI parameters (RD, FA and MD) sensitive to detect differences in regions with coherent fiber arrangement (the corpus callosum and anterior limb of internal capsule). Kurtosis parameters (MK and axial kurtosis (AK)) sensitive to differences in regions with complex fiber arrangement (juxtacortical white matter and corona radiata).
Zhu et al. (2016)	DKI and DTI	TBSS	19 schizophrenia patients with severe delusions (7 F/12 M; 34.6 years (9.4) 30 patients without delusions (16 F/14 M; 35.9 years (9.2)) 30 healthy controls (15 F/15 M; 35.3 years (9.3))	Lower FA in patients with delusions in comparison to both healthy controls and patients with severe delusions, including the genu and splenium of corpus callosum, anterior corona radiata and the optic radiation. Lower FA in patients without delusions, compared to healthy controls only, in the body of the corpus callosum and the superior corona radiata. Lower FA in patients without delusions in the inferior longitudinal fasciculus and the optic radiation in comparison to patients with severe delusions Patients with severe delusions demonstrated comparable FA in all of these white matter regions.
Narita et al. (2016)	DKI	Voxel-based	31 patients with schizophrenia (16 M/15 F; 40.3 years (8.9)) 31 healthy controls (15 M/16 F; 36.8 years (6.9))	More widespread MK reductions observed in schizophrenia, compared to FA measures Lower MK for patients observed in left limbic lobe, frontal lobe, parietal lobe, bilateral SLF, right posterior and anterior corona radiata. MK of left superior longitudinal fasciculus negatively correlated with the severity of positive symptoms No significant correlations between FA and clinical measures.
Docx et al. (2017)	DKI and DTI	Voxel-based	20 schizophrenia patients (18 M/2 F; 32.55 years (8.21)) 16 healthy controls (13 M/3 F; 30.56 years (6.73))	Motor activity level positively correlated with MK in the inferior, medial and superior longitudinal fasciculus, the corpus callosum, the posterior fronto-occipital fasciculus and the posterior cingulum for patients No significant associations observed for healthy controls or for conventional DTI measures
Zhao et al. (2016)	DKI and DTI	ROI	35 bipolar patients (18 M/17 F; 30.31 years (10.07)) 30 unipolar depression (UD) patients (13 M/17 F; 31.9 years (9.28)) 45 healthy controls (22 M/23 F; 31.91 years (11.73))	In the superior cerebellar peduncles (SCP), the UD group showed significantly increased axial kurtosis (Ka), mean diffusivity (MD) and decreased radial diffusivity (Dr) (compared with the HC group). MD values were lower in the UD group than in the bipolar group in the right SCP. In the middle cerebellar peduncles (MCP), the UD group showed significantly increased axial diffusivity (Ka) and decreased FA in bilateral MCP and increased Dr in the right MCP compared with the HC group. The BD group showed significantly

Study	Measure	Analysis method	Sample	Results
				decreased FA and increased Dr in the right MCP compared with the HC group. In the DN, the BD group showed significantly decreased MK in the left DN compared with the HC group.
Pasternak et al. (2012)	FW	TBSS	18 first-episode psychosis patients (4 F/14 M, 21.61 years (4.34)) 20 healthy controls (5 F/15 M; 24.05 years (3.99))	Higher extracellular volume of gray and white matter in first-episode schizophrenia. Lower FW-corrected FA limited to regional specific areas, mainly in the frontal lobe white matter
Lyall et al. (2017)	Q-ball	TBSS	70 healthy controls (24 M/46 F; 21.51 years (5.01) 63 FE patients (46 M/17 F; 21.38 years (4.86))	Lower FA across the whole brain in patients compared to healthy controls that overlap with significant increases in FW, with only limited decreases in free-water corrected FA. Higher FW correlated with better neurocognitive functioning following 12 weeks of antipsychotic treatment.
Pasternak et al. (2015)	FW	TBSS	29 chronic schizophrenia patients (4 F/25 M, 46.59 years (9.504)) 25 healthy controls (5 F/20 M; 43.68 years (7.62))	Widespread FW-corrected FA reductions in patients Elevated extracellular volume was more limited
Oestreich et al. (2017)	FW	TBSS	193 healthy controls (38.75 years; 47.4% male) 287 schizophrenia patients (39.80 years; 74% male)	Reduced FA for chronic schizophrenia group in the anterior limb of the internal capsule bilaterally, the posterior thalamic radiation bilaterally, as well as the genu and body of the corpus callosum. Significant main effect of group was observed for FW but none of the follow-up contrasts survived correction for multiple comparisons.
Oestreich et al. (2016)	FW	Tract-based	86 schizophrenia patients (34 present state delusions 37.94 years (9.77); 85% male) 35 lifetime history but currently remitted delusions (37.94 years (9.77) 77% male) 17 never experienced delusions) (41.12 years (11.97) 65% male) 28 healthy controls (37.86 years (9.66) 86% male)	Higher extracellular free-water in left cingulum bundle in association with present state delusions in chronic schizophrenia Present state and remitted delusions associated with reduced FA and increased MD in the cingulum. No significant differences in diffusion measures of the fornix and the uncinate fasciculus were observed
Mandl et al. (2015)	FW and MTR	Tract-based	40 schizophrenia patients (26.8 years (5.8)) 40 healthy controls (28.0 years (7.7))	Higher average MTR values observed in patients for the right uncinate fasciculus, the right arcuate fasciculus and the right inferior-frontal occipital fasciculus. No significant differences for diffusion measures were observe
Tuzzo et al. (2017)	FW		17 bipolar patients (16 M/12 F; 26.32 years (6) 28 healthy controls (8 M/9 F; 32.41 years (7.62))	lower FA in bipolar patients when compared to HC in regions that overlapped with extensive FW increases, including genu, body, and splenium of the corpus callosum, bilateral posterior limb of the internal capsule, bilateral corona radiata, bilateral external capsule and bilateral superior longitudinal fasciculus. There were no FA-t differences.
Bergamino et al., 2016	FW	TBSS	16 female major depression patients (40.1 years (10.6)) 16 female healthy controls (34.8 years (11.8))	After applying free-water correction, MDD patients had significantly decreased FA and axial diffusivity (AD) in the left inferior frontooccipital fasciculus (IFOF) and increased self-reported stress that significantly correlated with decreased IFOF AD in depression.
Wang et al. (2016)	FW	TBSS	87 individuals at risk for psychosis (58 M/29 F; 21.5 years (3.6))	Reduced FA in left cingulum, corpus callosum, left uncinate fasciculus, forceps minor, left inferior frontooccipital fasciculus, left

Study	Measure	Analysis method	Sample	Results
			37 healthy controls (20 M/17 F; 23.2 years (4))	superior longitudinal fasciculus, and left anterior thalamic radiation for high risk group Reduced axial diffusivity for high risk group in cingulum and corpus callosum FA correlated with symptom severity FA of forceps minor further reduced in subjects who transitioned to psychosis after 2 years.
Kochunov et al. (2013)	PDI and DTI	TBSS	26 schizophrenia patients (7 F/19 M; 39.9 years (12.8)) 27 healthy controls (12 F/15 M) 37.5 years (11.9))	Lower PDI in the CC and cingulate grey matter of patients, with more modest differences in FA.
Kochunov et al. (2014)	PDI and DTI	TBSS	30 schizophrenia patients (21 M/9 F; 40.1 years (12.1)) 40 healthy controls (23 M/17 F; 41.9 years (12.9))	Lower corpus callosum FA for patients and age-by-diagnosis interaction Lower PDI for patients in the same region but no difference in hyperintensive white matter (HWM) lesions. PDI and HWM volume were significant predictors of FA and explained the variance that was associated with diagnosis. Variance in FA due to age, diagnosis, and diagnosis-by-age interaction, accounted for by HWM volume and a PDI-by-diagnosis interaction Accelerated decline in FA of schizophrenia patients also explained by decline in PDI
Kochunov et al. (2016)	DKI, PDI, DTI	Voxel-based	74 schizophrenia patients (54M/20F; 40.0 years (11.6)) 41 healthy siblings (14 M/27 F; 38.9 years (14.9)) 113 healthy controls (76 M/37 F; 41.0 years (11.9))	Significant differences between patients and controls across four measures (FA, kurtosis anisotropy (KA), axial kurtosis (KII), and PDI). FA, KA, and PDI showed significant differences between controls and siblings. Diffusion parameters that showed significant patient-control differences also explained patient-control differences in processing speed. This association was also found for siblings The association was specific to processing-speed abnormality but not working memory or psychiatric symptoms
Rae et al. (2017)	NODDI	TBSS	35 first-episode psychosis patients (27 M/8 F; 26.9 years) 19 healthy controls (13 M/6 F; 24.7 years)	Lower regional FA for first-episode patients in multiple commissural, corticospinal, and association tracts. Differences in FA co-localized with regions of reduced neurite density, rather than orientation dispersion index (ODI)
Nazeri et al. (2016)	NODDI		36 schizophrenia patients (17 F/19 M; 35.5 years (8.4)) 29 bipolar I patients (15 F/14 M; 31.5 years (11.0)) 35 healthy controls (16 F/19 M; 33.6 years (12.4))	Lower grey matter neurite orientation dispersion (NDI) in temporal pole, anterior parahippocampal gyrus, and hippocampus of schizophrenia patients compared to healthy controls No significant differences in grey matter NDI between bipolar I patients, schizophrenia patients or healthy controls. Spatial working memory associated with higher GM-NDI mainly in DLPFC, orbitofrontal, medial prefrontal, superior temporal, and cingulate cortices; and temporal pole, insula, hippocampus, and striatum Addition of grey matter NDI to cortical thickness resulted in higher accuracy to predict group membership
Westin et al. (2016)	Q-ball q-space trajectory imaging (QTI)	Voxel-based	5 schizophrenia patients 5 healthy controls	9 out of the 14 parameters investigated showed differences between groups, including MD, V_{MD}, C_μ, CM, μFA, FA, Kbulk, Kshear, K_μ

Author Manuscript

Author Manuscript

Author Manuscript

Author Manuscript

Table 2:

Summary table of technical parameters

Study	Measure	Scanner	Scheme	Max b-value (s/mm^2)	directions (b=0)	Resolution (mm^3)	TR/TE (ms)
Mendelsohn et al (2006)	QSI and DTI	1.5T	15 shells	14000	6*15(6)	1.9×1.9×5	2000/167
Huang et al. (2010)	GFA	3T	Modified DSI-203	4000	102(not indicated)	2.5×2.5×2.5	9100/142
Huang et al. (2011)	GFA	3T	Modified DSI-203	4000	102(not indicated)	2.5×2.5×2.5	9100/142
Wu et al. (2014)	GFA	3T	Modified DSI-203	4000	102(not indicated)	2.5×2.5×2.5	9600/130
Wu et al. (2015a)	GFA	3T	Modified DSI-203	4000	102(not indicated)	2.5×2.5×2.5	9600/130
Wu et al. (2015b)	GFA	3T	Modified DSI-203	4000	102(not indicated)	2.5×2.5×2.5	9600/130
Tseng et al. (2015)	GFA	3T	Modified DSI-203	4000	102(not indicated)	2.5×2.5×2.5	9600/130
Griffa et al. (2015)	GFA	3T	DSI	8000	128(1)	2.2×2.2×3	6100/144
Katz et al. (2016)	GFA	3T	Single shell	1400	60(1)	2×2×2	not indicated
Baumann et al. (2016)	GFA	3T	DSI	8000	128(1)	2.2×2.2×3	6800/144
Rathi et al. (2010)	GFA	3T	Single shell	900	51(8)	1.66 ×1.66 × 1.7	not indicated
Sarrazin et al. (2014)	GFA	3T	Single shell	1000	40(1)	2×2×2	14000/84 or 14000/87
Scholz et al. (2016)	GFA	3T	Single shell	not indicated	61(3)	1.8×1.8×1.8	11000/88.8
Favre et al. (2016)	GFA, MD	3T	single shell	1400	30(not indicated)	not indicated	not indicated
Souza-Queiroz et al. (2016)	GFA	3T	Single shell	1400	60(1)	2×2×2	12000/92
Canales-Rodriguez (2014)	GFA and DTI	1.5T	single shell	1500	55(1)	2.2×2.2×3	16675/100.2
Chen et al. (2016)	GFA	1.5T	3 shells	2000	25×3(4)	2×2×4	10500/120
Ramani et al. (2007)	DKI and DTI	3T	5 shells	2500	30×5(30)	2×2×4	2300/109
Zhu et al. (2015)	DKI and DTI	3T	2 shells	2000	25×2(10)	2×2×3	5800/77
Zhu et al. (2016)	DKI and DTI	3T	2 shells	2000	25×2(10)	2×2×3	5800/77
Narita et al. (2016)	DKI	3T	2 shells	2000	32×2(32)	3×3×3	5032/85
Docx et al. (2017)	DKI and DTI	3T	3 shells	2800	25 at b=700, 40 at b=1000, 75 at b=2800 (10)	2.2×2.2×2.2	7700/139
Zhao et al. (2016)	DKI	3T	5 shells	2500	15×5(15)	2×2×2	4500/min
Pasternak et al. (2012)	FW	3T	single shell	900	51(8)	1.7×1.7×1.7	17000/~86
Lyall et al. (2017)	FW	3T	single shell	1000	31(5)	2.5×2.5×2.5n ot indicated	14000/84.8
Pasternak et al. (2015)	FW	3T	single shell	900	51(8)	1.7×1.7×1.7	17000/~86

Study	Measure	Scanner	Scheme	Max b-value (s/mm^2)	directions (b=0)	Resolution (mm^3)	TR/TE (ms)
Oestreich et al. (2017)	FW	1.5T	single shell	1000	64(1)	2.4×2.4×2.5	84000/88
Mandl et al. (2015)	FW and MTR	1.5T	single shell	1000	32(8)	2.5×2.5×2.5	9822/88
Oestrich et al. (2016)	FW	1.5T	single shell	1000	64(1)	2.4×2.4×2.4	8400/88
Tuozzo et al. (2017)	FW	3T	single shell	1000	12(1)	2.5×2.5×2.5	8500/89
Bergamino et al. (2016)	FW	3T	single shell	1000	30(1)	not indicated	8800/78.1
Wang et al. (2016)	FW	3T	single shell	1000	30(2)	2×2×2	9600/107
Kochunov et al. (2013)	PDI	3T	15 shells	3800	30×15(16)	1.7×1.7×4.6	1500/120
	DTI	3T	single shell	700	64(5)	1.7×1.7×3	8000/87
Kochunov et al. (2014)	PDI	3T	15 shells	3800	30×15(16)	1.7×1.7×4.6	1500/120
	DTI	3T	single shell	700	64(5)	1.7×1.7×3	8000/87
Kochunov et al. (2016)	DKI, PDI, DTI	3T	15 shells	3,800	30×15(16)	1.7×1.7×4.6	1500/120
Rae et al. (2017)	NODDI	1.5T	3 shells	2400	9 at b=300, 30 at b=800, 60 at b=2400 (11)	2.5×2.5×2.5	8400/99
Nazeri et al. (2016)	NODDI	3T	3 shells	4500	30×3(5)	2×2×2	12000/108
	DTI	3T	single shell	1000	60(5)	2×2×2	8800/85
Westin et al. (2016)	QTI	3T	5	2000	216(6)	3×3×3	6000/160

Table 3:

List of abnormal brain locations that were identified in the reviewed studies.

Region	Measure	Schizophrenia	Bipolar	MDD
Cingulate	gFA	Huang et al. (2010); Huang et al. (2011)	Sarrazin (2014); Scholz (2016); Canales-Rodnguez (2014)	
	DKI	Docx et al. (2017)		
	FA$_T$	Oestreich et al. (2016); Wang et al. (2016)		
	PDI	Kochunov et al. (2013)		
Corpus callosum	gFA	Wu et al. (2015a); Wu et al. (2015b)	Sarrazin (2014); Canales-Rodnguez (2014)	Chen et al. (2016b)
	DKI	Zhu et al. (2015); Docx et al. (2017)		
	FW	Lyall et al. (2017)	Tuozzo et al. (2017)	
	FA$_T$	Pasternak et al. (2015); Oestreich et al. (2017) Wang et al. (2016)		
	NODDI	Rae et al. (2017)		
	PDI	Kochunov et al. (2013); Kochunov et al. (2014)		
Uncinate	gFA		Favre (2016); Souza-Queiroz (2016)	
	FA$_T$	Wang et al. (2016)		
Fornix	gFA	Wu et al. (2015a); Wu et al. (2015b); Baumann et al. (2016)		
Inferior longitudinal fasciculus	DKI	Docx et al. (2017)		
Inferior fronto-occipital fasciculus	gFA	Wu et al. (2015a); Katz et al. (2016)		
	FW	Mandl et al. (2015); Wang et al. (2016); Pasternak et al. (2012)		Bergamino et al. (2016)
Superior longitudinal fasciculus	gFA	Wu et al. (2015a)		Chen et al. (2016b)
	DKI	Docx et al. (2017)		
	FW	Pasternak et al. (2012); Lyall et al. (2017)	Tuozzo et al. (2017)	
	FA$_T$	Wang et al. (2016);		
Arcuate	gFA	Wu et al. (2015a); Wu et al. (2015b)	Sarrazin (2014); Sarrazin (2013)	
Corona radiata	DKI	Zhu et al. (2015); Narita et al. (2016)		
	FW	Lyall et al. (2017)	Tuozzo et al. (2017)	
	FA$_T$	Pasternak et al. (2015);		
Internal/external capsule	DKI	Zhu et al. (2015)		

Region	Measure	Schizophrenia	Bipolar	MDD
	FW		Tuozzo et al. (2017)	
	FA_T	Oestreich et al. (2017); Pasternak et al. (2015)		
Temporal	gFA	Wu et al. (2015a); Wu et al. (2015b); Wu et al. (2014)		
	FA_T	Pasternak et al. (2015)		
	NODDI	Nazeri et al. (2016)		
Frontal	gFA	Wu et al. (2015); Wu et al. (2014); Tseng et al. (2015)		
	DKI	Ramani et al. (2007)		
	FW	Pasternak et al. (2012)		
	FA_T	Pasternak et al. (2015)		
	NODDI	Nazeri et al. (2016)		
	QSI	Mendelsohn et al. (2006)		
	NQA			Chen et al. (2016b)
Parietal	gFA	Huang et al. (2010)		
	DKI	Narita et al. (2016)		
	FA_T	Pasternak et al. (2015)		
Thalamic radiation	FA_T	Pasternak et al. (2015)		
Cerebellar peduncles	DKI		Zhao et al. (2016)	Zhao et al. (2016)
	FA_T	Pasternak et al. (2015)		